

**Gelation and Rheological Properties of Ultrasound-  
Extracted Faba Bean Protein: A Comparative Study with  
Commercial Plant Proteins**

BADJONA, Abraham, CHERONO, Beatrice, BRADSHAW, Robert and  
DUBEY, Bipro <<http://orcid.org/0000-0003-0396-9864>>

Available from Sheffield Hallam University Research Archive (SHURA) at:

<https://shura.shu.ac.uk/34610/>

---

This document is the Published Version [VoR]

**Citation:**

BADJONA, Abraham, CHERONO, Beatrice, BRADSHAW, Robert and DUBEY, Bipro (2024). Gelation and Rheological Properties of Ultrasound-Extracted Faba Bean Protein: A Comparative Study with Commercial Plant Proteins. *Food Hydrocolloids*: 110997. [Article]

---

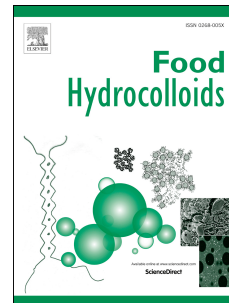
**Copyright and re-use policy**

See <http://shura.shu.ac.uk/information.html>

# Journal Pre-proof

Gelation and Rheological Properties of Ultrasound-Extracted Faba Bean Protein: A Comparative Study with Commercial Plant Proteins

Abraham Badjona, Beatrice Cheronon, Robert Bradshaw, Bipro Dubey



PII: S0268-005X(24)01271-2

DOI: <https://doi.org/10.1016/j.foodhyd.2024.110997>

Reference: FOOHYD 110997

To appear in: *Food Hydrocolloids*

Received Date: 26 October 2024

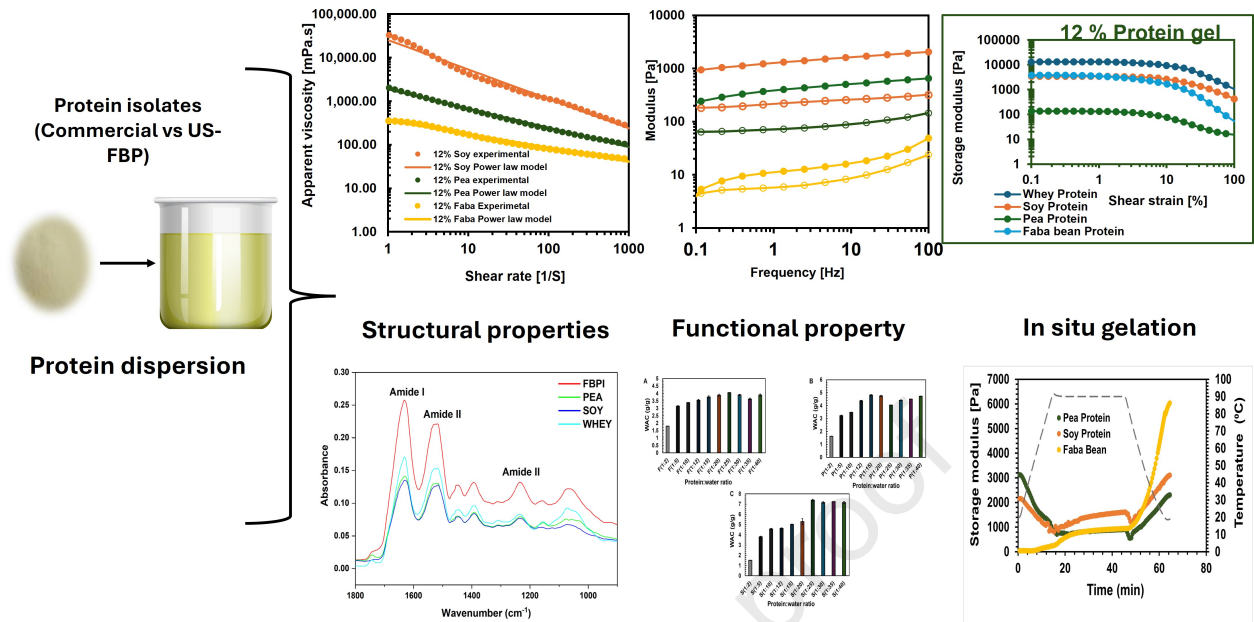
Revised Date: 3 December 2024

Accepted Date: 16 December 2024

Please cite this article as: Badjona, A., Cheronon, B., Bradshaw, R., Dubey, B., Gelation and Rheological Properties of Ultrasound-Extracted Faba Bean Protein: A Comparative Study with Commercial Plant Proteins, *Food Hydrocolloids*, <https://doi.org/10.1016/j.foodhyd.2024.110997>.

This is a PDF file of an article that has undergone enhancements after acceptance, such as the addition of a cover page and metadata, and formatting for readability, but it is not yet the definitive version of record. This version will undergo additional copyediting, typesetting and review before it is published in its final form, but we are providing this version to give early visibility of the article. Please note that, during the production process, errors may be discovered which could affect the content, and all legal disclaimers that apply to the journal pertain.

© 2024 Published by Elsevier Ltd.



1 **Gelation and Rheological Properties of Ultrasound-Extracted Faba Bean Protein: A**  
2 **Comparative Study with Commercial Plant Proteins**

3 **Abraham Badjona<sup>1</sup>, Beatrice Cheron<sup>1</sup> Robert Bradshaw<sup>2</sup>, Bipro Dubey<sup>1,3\*</sup>**

4 <sup>1</sup>National Centre of Excellence for Food Engineering, Sheffield Hallam University, Sheffield,  
5 S1 1WB, [a.badjona@shu.ac.uk](mailto:a.badjona@shu.ac.uk) (A.B), [beatricecheronob@gmail.com](mailto:beatricecheronob@gmail.com), [b.dubey@shu.ac.uk](mailto:b.dubey@shu.ac.uk)  
6 (B.D)

7 <sup>2</sup>Bimolecular Research Centre, Sheffield Hallam University, Sheffield, S1 1WB, UK;  
8 [r.bradshaw@shu.ac.uk](mailto:r.bradshaw@shu.ac.uk) (R.B)

9 <sup>3</sup>School of Engineering and Built Environment, College of Business, Technology and  
10 Engineering, Sheffield Hallam University, Sheffield, S1 1WB, UK.

11 \*Correspondence: [b.dubey@shu.ac.uk](mailto:b.dubey@shu.ac.uk) (B.D)

12 **ABSTRACT**

13 Environmental and consumer concerns about dependence on animal-based proteins have  
14 sparked interest in sustainable alternatives, with plant-based biopolymers emerging as a  
15 promising substitute. The present study comprehensively assessed and compared the  
16 rheological and structural properties of commercial plant proteins (pea and soy) and  
17 ultrasound-extracted faba bean protein (US-FBP) to provide an extensive overview of their  
18 comparative characteristics. At 12 % protein concentration, the exponent  $n$  approached zero for  
19 soy ( $n = 0.32$ ) and pea ( $n = 0.56$ ), whereas it remained higher for faba bean protein ( $n = 0.69$ )  
20 after fitting a viscosity curve to power law model. The least gelation concentration was  
21 observed to be 10 % for US-FBP, soy and pea protein. Additionally, in situ gelation indicated  
22 strong gel formation by soy (loss factor = 0.19) compared to US-FBP (0.24) and pea protein  
23 (0.37). Secondary structure analysis using FTIR spectroscopy and water/oil absorption capacity  
24 measurements revealed significant differences between these proteins. This opens interesting

25 possibilities for using a wide range of plant proteins in the design, formulation, and  
26 customization of next-generation plant-based foods.

27

28 **Keywords:** Rheology, gelation, plant protein, biopolymer, plant-based foods, ultrasound-  
29 extracted faba bean protein (US-FBP).

30

### 31 **Introduction**

32 The interest in the plant-based food industry is gaining increasing attention with plant-derived  
33 alternatives to standard meat and dairy products becoming established options. Research has  
34 demonstrated that plant-based diets, which include plant proteins, can provide significant  
35 nutritional benefits while also enhancing environmental sustainability (Magrini et al., 2018).

36 The health benefits associated with consumption of plant-based diets are notable and are key  
37 areas of scientific interest. Lescinsky et al., (2022) revealed that diets characterized as  
38 vegetarian and prudent, which include small quantities of red meat, are correlated with a  
39 reduced risk of diseases, notably heart disease and type 2 diabetes. The production of food  
40 through livestock farming significantly contributes to emissions of greenhouse gases, depletion  
41 and degradation of resources, and biodiversity losses (Hayek et al., 2021). Annually, billions  
42 of animals are bred and slaughtered for food, frequently experiencing unfavourable conditions  
43 (Weathers et al., 2020). Large-scale animal production in factory farms heightens the danger  
44 of zoonotic diseases and antibiotic resistance, posing a significant threat to both the global  
45 economy and public health (Stevenson, 2023). Despite the increase in plant-based alternatives  
46 in many countries, the consumption of animal-based proteins remains predominant.

47 Presently, the majority of proteins utilized as functional ingredients in plant-based foods are  
48 derived from a limited number of sources, including soybeans, peas, wheat, and corn.

49 Nonetheless, many other protein sources can be utilized to formulate these products, potentially  
50 providing new or improved functional properties, such as thickening and gelling agents as well  
51 as for foaming or emulsifying (Paximada et al., 2021). For example, proteins displaying these  
52 functional characteristics can be extracted from faba beans (Badjona et al., 2024c), tubers, nuts,  
53 cereals (Kaur et al., 2022) and a variety of other sources. Globulins are the major storage  
54 proteins of pulses constituting between 35 and 80 % of the total protein content. The major  
55 structural composition and functionality of different pulse globulins has been extensively  
56 investigated in previous research (Sim et al., 2021) and have been shown to have numerous  
57 applications in the food industry. Moreover, it is now apparent that isolation methods and  
58 downstream processing can alter the functionality of plant proteins, resulting in isolates with  
59 the same [percent/level] of protein but displaying very different properties (Schlangen et al.,  
60 2022a). The protein source is also a determinant factor defining the textural properties of milk  
61 and meat analogues that drives consumer preferences (McClements, 2023). For instance, soy  
62 protein and wheat gluten provide a more fibrous structure and elastic texture than pea protein  
63 (Snel et al., 2022). However, since wheat and soy are major food allergens (Coimbra et al.,  
64 2023), the use of pulse proteins, e.g., peas, mung beans, and fava beans, is recently gaining  
65 importance (Badjona et al., 2023; Mazumder et al., 2023).

66 The apparent viscosity of suspensions in high-moisture biopolymer systems has been used to  
67 elucidate structure-function relationships (McClements, 2023; McClements et al., 2019). The  
68 viscoelastic and gelling properties of globular proteins are influenced by numerous complex  
69 factors, making a thorough understanding of these interactions essential for food applications.  
70 Rheological properties, including shear viscosity for fluids and elastic modulus and fracture  
71 properties for solids, significantly affect the production quality, storability, and sensory aspects  
72 of next-generation plant-based foods (Kyriakopoulou et al., 2019). Conversely, using plant-  
73 based proteins from various sources as gelling agents can enhance overall sustainability,

74 provide broader functionality in gelation, water-holding capacity, and emulsification, offer  
75 consumers a wider selection, and provide health benefits (Ma, Greis, et al., 2022a). The  
76 necessity for a deeper understanding in this field is emphasized by the observation that many  
77 consumers attribute their low acceptance of plant-based analogues to undesirable textural and  
78 sensory qualities (Michel et al., 2021).

79 The functional performance of various plant proteins can differ significantly between suppliers  
80 and batches (Jiménez-Munoz et al., 2023), complicating the formulation of commercial food  
81 products with consistent quality attributes. Therefore, this article focuses on understanding,  
82 predicting, and controlling the rheological characteristics of next-generation plant-based foods  
83 by: (i) investigating protein systems in the dilute biopolymer regime using viscosity  
84 measurements, (ii) analysing the viscoelastic behaviour of different protein dispersions, (iii)  
85 studying the minimum gelation concentration, (iv) examining the gelation mechanism through  
86 temperature sweeps, and (v) elucidating structural differences and water-holding capacity. This  
87 knowledge is expected to provide new opportunities for the diverse use of plant proteins in the  
88 development, design, and production of higher-quality plant-based products.

## 89 **Materials and Method**

### 90 **Raw Materials and Chemicals**

91 Faba beans were sourced from Whole Foods Earth (Kent, United Kingdom). Sodium hydroxide  
92 (NaOH,  $\geq 99.9$  % purity) and hydrochloric acid (37 %) (HCl) were obtained from Sigma-  
93 Aldrich (UK). The seeds were finely milled using a Retsch twister cyclone mill at 12,000 rpm  
94 (sieve size of 0.5 mm) and stored at  $-20$  °C until required. The particle size of the milled flour  
95 can be found in our previous work (Badjona et al., 2024c). Three different commercial proteins  
96 were procured from various suppliers: pea and soy protein isolates from Pulsin Co. Limited  
97 (UK) and whey protein isolate from Myprotein (UK) as shown in **Table 1**.

98

99 **Table 1.** Chemical composition of plant protein used in this work.

Protein	Fat (%)	Carbohydrate (%)	Fibre (%)	Protein (%)	Salt (%)	Source
Soy	1.5	1.8	-	90	0.5	Plant (commercial)
Pea	9.1	0.2	1.4	80	4.90	Plant (commercial)
Whey	7.5	4.0	-	82	0.50	Animal (commercial)
US-FBP	nd	nd	nd	92	nd	Plant (Laboratory)

100 NB: Whey contained Soya lecithin and sunflower lecithin emulsifiers. nd: not determined.

### 101 Preparation of Protein solutions

102 Pea, US-FBP, and soy proteins were dissolved in deionized water to obtain stock solutions at  
 103 12 and 10 % (w/v) concentration at 4 °C and stirred gently with a magnetic stirrer overnight.  
 104 Within the first 2 hours, the pH was adjusted to 7 using 1 M NaOH or HCl. The protein  
 105 solutions were then diluted from the stock solution to concentrations of 10, 7, 5, and 4 %, with  
 106 the pH readjusted to 7 after dilution (**Table 2**). The samples were prepared based on protein  
 107 mass fraction.

108 **Table 2.** Nomenclature and formulation of protein suspensions from soy, pea and faba bean  
 109 proteins.

Protein	Protein mass concentration (w/v %)	Total mass fraction (g)	Aqueous (mL)
Soy	12	13.33	86.67
	10	11.11	88.89
	7	7.78	92.22
	5	5.56	94.44
	4	4.44	95.56
Pea	12	15	85
	10	12.5	87.50



	7	8.75	91.25
	5	6.25	93.75
	4	5	95
US-FBP	12	13.04	89.96
	10	10.87	89.13
	7	7.61	92.39

110

111

### 112 **Extraction of ultrasound-assisted faba bean protein isolate**

113 Under the optimal conditions—power of 123 W, solute/solvent ratio of 0.06 (1:15 g/mL),  
 114 sonication time of 41 minutes, and total volume of 623 mL—yielded a maximum extraction  
 115 efficiency of 19.75 % and a protein content of 92.87 %, as established in a previous study  
 116 (Badjona et al., 2024a, 2024b). For this study, faba bean flour was dispersed in water at a  
 117 solute/solvent ratio of 0.06 (1:15 g/mL) with a total volume of 623 mL. The dispersion was  
 118 agitated at 25 °C for 20 minutes at 500 rpm prior to ultrasonic-assisted extraction. The pH was  
 119 adjusted to 11, followed by ultrasonic treatment at 123 W for 41 minutes using a S24d22D  
 120 titanium ultrasonic horn (Teltow, Germany). The temperature was maintained between 20 and  
 121 25 °C using an ice bath. The mixture was then centrifuged at 25 °C for 20 minutes at 6,000 rpm  
 122 using an accuSpin™ 400 centrifuge (United Kingdom). The supernatant was collected, and  
 123 the pH was adjusted to 4.0 with 1 N HCl while stirring continuously for 20 minutes. Protein  
 124 isolate pellets were obtained by centrifugation at 6,000 rpm for 20 minutes at 25 °C. The protein  
 125 pellets were lyophilized for 48 hours and stored at -20 °C for further analysis.

### 126 **Viscosity**

127 Protein samples were prepared as described previously and a concentration range between 12  
 128 and 4 % was used for measurement. Small deformation rheology was conducted using a  
 129 rotational rheometer (MRC 302, Anton Paar, Graz, Austria) equipped with a 17 mm by 43 mm  
 130 concentric cylinder with a gap of 1 mm (CC17/T200/SS) and an attached vane geometry  
 131 (SR15-2V/2 V-32/100). The unit was temperature-controlled at 20°C using an integrated water

132 bath. Suspensions were added to fill the concentric cylinder to its maximum volume, and the  
 133 viscosity of the samples was measured through a shear sweep ranging from 0.01 to 1500 s<sup>-1</sup>.  
 134 Each sample was analysed in replicates (n = 4), and the data was processed using RheoCompass  
 135 Software. Data was fitted to the power law model,

136 Apparent viscosity was calculated by the equation with the assumption that yield stress = 0,

$$137 \quad \mu_{\text{app}} = K\dot{\gamma}^{(n-1)} \dots \text{eq. (1)}$$

138 where  $\mu_{\text{app}}$  represents apparent viscosity (Pa·s),  $K$  is the consistency coefficient (Pa·s),  $\dot{\gamma}$  is the  
 139 shear rate (s<sup>-1</sup>), and  $n$  is the flow behaviour index. Applying the log function to eq. (1),  
 140 natural logarithm (ln) of both sides of equation 1:

$$141 \quad \ln \mu_{\text{app}} = \ln K + \ln \dot{\gamma}^{n-1} \dots \text{eq. (2)}$$

$$142 \quad \ln \mu_{\text{app}} = \ln K + (n - 1)\ln \dot{\gamma} \dots \text{eq. (3)}$$

143 Eq. (3) is a linear equation considering  $\ln \dot{\gamma}$  and  $\ln \mu_{\text{app}}$  are independent (x) and dependent (y)  
 144 variable, where  $\ln K$  and  $(n-1)$  represents intercept and slope respectively.  $K$  (the consistency  
 145 parameter) and  $n$  (flow behaviour index) can be estimated from experimental data.

146

### 147 **Oscillatory measurement: Amplitude sweep**

148 Amplitude scanning was initially conducted to identify the linear viscoelastic region (LVR) of  
 149 12-20 wt.% protein dispersions. A strain-sweep experiment was carried out at a constant  
 150 frequency of 0.1 and 1 Hz at 20 °C. The storage modulus ( $G'$ ) and loss modulus ( $G''$ ) were  
 151 measured across a strain range of 0.1–1000 % to determine the LVR for the different protein  
 152 isolates.

153

**154 Oscillatory measurement: Frequency sweep**

155 Small-amplitude oscillatory shear experiments were performed over an angular frequency ( $\omega$ )  
156 range of 0.1–100 Hz at a constant strain rate of 0.2 % and a temperature of 20 °C, resulting in  
157 measurements of the storage modulus ( $G'$ ) and loss modulus ( $G''$ ). The strain amplitude of 0.2  
158 % was chosen based on the amplitude sweep tests and was within the linear viscoelastic (LVE)  
159 regime for all samples under investigation. Protein dispersion used for this measurement was  
160 12-20 wt.%.

**161 In situ gelation**

162 Protein dispersions at concentrations of 12 and 15 wt.% for rheometer testing were prepared as  
163 previously described. All samples were stirred overnight before rheological measurements. The  
164 rheological properties of the gels were tested using a rheometer equipped with a 17 mm by 43  
165 mm concentric cylinder and attached vane geometry. The protein dispersions were carefully  
166 poured into the cup until the sampling area was filled, then covered with a thin layer of paraffin  
167 oil and a solvent trap to prevent water evaporation. Various tests were subsequently conducted  
168 on the samples:

169 (1) Temperature sweep (Gelation test): This involved heating the samples from 20 to 90 °C  
170 at a rate of 5 °C/min, holding them at 90 °C for 30 minutes, and then cooling them back  
171 to 20°C at the same rate. The rheological parameters used to characterize the gels were  
172 the storage modulus ( $G'$ ), loss modulus ( $G''$ ), and the loss factor  $\tan \delta$  ( $G''/G'$ ).  $G'$  and  
173  $G''$  represent the elastic and viscous components of the viscoelastic behaviour,  
174 respectively, while  $\tan \delta$  describes the ratio of these two components. A material is  
175 considered a solid when  $\tan \delta < 1$  and a strong solid when  $\tan \delta \ll 1$ .

176 (2) Frequency sweep: the final gels were analysed using a frequency sweep spanning from  
177 1 to 100 Hz, at a constant strain of 0.2 %.

178 (3) Strain sweep: a strain sweep was conducted while maintaining a constant temperature  
179 of 20 °C and a frequency of 1 Hz, with the strain ranging from 0.1 to 1000 %.

### 180 **Least gelation concentration.**

181 The least gelation concentration was determined using a modified version of the method  
182 described by Kamani et al., (2024). Protein suspensions of varying concentrations (2, 4, 5, 7,  
183 10, 12, 15 and 20 %) at pH 7 were prepared with a total volume of 20 mL each protein basis  
184 was used. The samples were then heated at 90 °C for 1 hour, followed by cooling under running  
185 tap water. The cooled samples were subsequently incubated in the refrigerator (4 °C) for about  
186 12 hrs. After gelation, a strain sweep was conducted while maintaining a constant temperature  
187 of 20 °C and a frequency of 1 Hz, with the strain ranging from 0.1 to 100 % to characterize the  
188 different gel strengths. Heat-set gels (12, 15 and 20 wt.%) were placed on a rotational rheometer  
189 (MRC 302, Anton Paar, Graz, Austria) equipped with a parallel plate and a gap of 1 mm was  
190 used for strain sweep measurement.

191

### 192 **Protein water holding capacity (WHC).**

193 **Water holding** capacities were measured using a modified version of the method by Yang et  
194 al., (2023). Faba bean protein isolate (1.0 g) was dispersed in varying distilled water volumes  
195 (2, 5, 10, 12, 15 and 40 mL). The mixtures were vortexed for 1 min on maximum speed and  
196 allowed to stand for 2 hr at room temperature (20 – 23 °C). Afterwards, the samples were  
197 centrifuged at 3000 x g for 15 min at 20 °C and the WHC was estimated using eq. (4).

198

199 
$$WHC = \frac{w_0 - w_1}{w_3} \times 100 \% \dots\dots \text{eq. (4)}$$

200 Where  $w_0$  is the mass of the tube and protein isolate and absorbed water;  $w_1$  is the mass of the  
201 tube and protein isolate while  $w_3$  is the mass of faba bean protein.

202

### 203 **Fourier-transform infrared spectroscopy analysis**

204 An Attenuated Total Reflectance (ATR)-FTIR spectrophotometer (Spectrum 100 FT-IR,  
205 PerkinElmer, USA) was employed for the FTIR analysis. Spectroscopic measurements were  
206 performed with 16 scans at a resolution of  $4\text{ cm}^{-1}$  over the range of  $4000 - 650\text{ cm}^{-1}$ .

### 207 **Statistical analysis**

208 All statistical analyses were performed by Origin 2019 and excel 2024 (version 2406). All the  
209 values were expressed as means  $\pm$  standard deviation (SD). All analysis was carried out in  
210 replicates except in situ gelation which was done in duplicate.

211

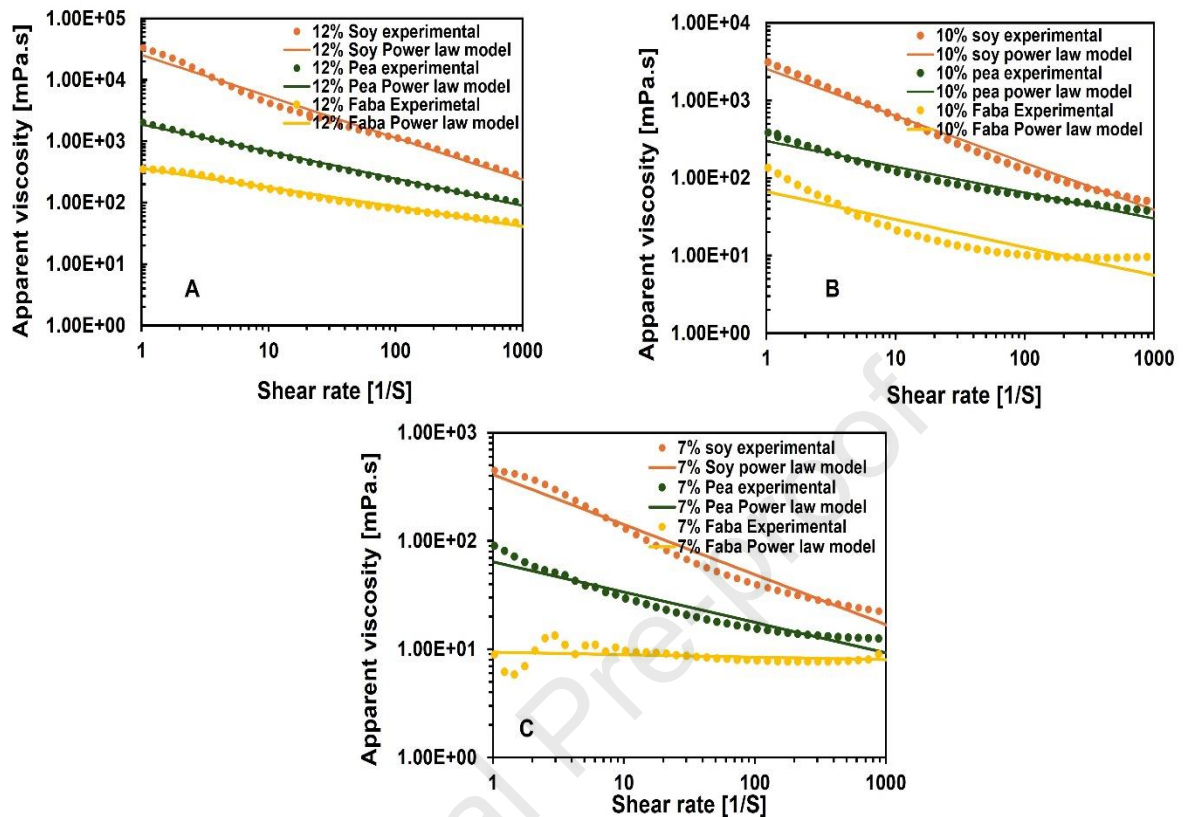
## 212 **RESULTS AND DISCUSSION**

### 213 **Viscosity**

214 The viscosity of biopolymer suspensions has been extensively studied to elucidate the  
215 structural and interactive dynamics within polymer mixtures (McClements, 2023). Additional  
216 studies are necessary to investigate the viscosity properties of different plant protein types.

217 Viscosity, which is the measure of a fluid's resistance to flow, is directly affected by  
218 concentration, the strength of molecular bonds, and the morphology of the molecules in the  
219 suspension (Benoit et al., 2013). In certain instances, the viscosity of nonideal fluids varies  
220 with the duration of applied shear stress (Ansari et al., 2020). The viscosity of protein  
221 suspensions was examined at various protein concentrations. The flow curves, representing  
222 viscosity as a function of shear rate for 12, 10, and 7 % solutions over a shear strain rate range  
223 of  $1$  to  $1000\text{ s}^{-1}$ , are depicted in **Fig. 1**. Although the overall flow curves differed across protein

224 concentrations, they all exhibited a shear-thinning behaviour. This trend aligns with other  
225 hydrocolloids reported in the literature and can be modelled using the power law equation. As  
226 illustrated in **Fig. 1**, the power law model fits reasonably for soy and pea proteins compared to  
227 faba bean proteins due to the complex structures of soluble and suspended proteins. At  
228 comparable protein concentrations, soy exhibited the highest viscosity, followed by pea  
229 protein, while faba bean protein suspensions demonstrated the lowest viscosity. In this present  
230 study, faba bean protein was found to have the lowest water-holding capacity compared to soy  
231 and pea proteins, which likely contributed to its reduced viscosity. Additionally, soy and pea  
232 proteins contain starch and fibre, which provide the structural integrity necessary to maintain  
233 viscosity even at low concentrations. The low viscosity of faba bean suspension could be  
234 advantageous for creating next-generation plant-based milk analogues with high protein  
235 content. Next generation plant based (NG-PB) milks typically consist of various particles or  
236 polymers suspended in an aqueous solution containing dissolved substances like sugars and  
237 salts. These products generally have a relatively low viscosity to mimic that of cow's milk  
238 (McClements, 2023; McClements & Grossmann, 2021).



240 **Fig. 1.** Viscosity flow curves investigating different protein concentration (w/v) suspension of  
 241 A) 12 % solution; B) 10 % solution; C) 7 % solution measured at 20 °C. Modelled with fits  
 242 from the power-law is presented as solid lines, respectively. Each point is the average of 4  
 243 replicates.

244 **Table. 3** illustrates the power law fitting parameters of the protein solutions measured across  
 245 the typical viscometer range of 1 to 1000  $s^{-1}$ . It is evident that viscosity is influenced by  
 246 polymer concentration. This analysis aimed to evaluate differences in flow behaviour and  
 247 estimate the  $K$  and  $n$  values within this range, providing insights for rheometers with limited  
 248 shear rate capabilities. All solutions exhibited shear-thinning behaviour, as indicated by the  
 249 power law index ( $n$ ) and consistency coefficient ( $K$ ). The reduction in viscosity with increasing  
 250 shear rate can be attributed to the entanglement theory. As shear stress causes disruption of the  
 251 protein molecular structure, interactions between adjacent chains diminish. This behaviour is  
 252 similar to that observed in certain milk or fluid egg analogues, where viscosity decreases with

253 increasing shear rate due to the disruption of particles or polymers held together by weak forces  
 254 (McClements et al., 2019). The model parameters for this range are summarized in **Table 3**.  
 255 Additionally, the apparent viscosity at  $100 \text{ s}^{-1}$  representing the average shear rate in a n extruder  
 256 for meat analogues is represented in **Table 3**.

257

258 **Table 3.** Power law model fitting parameters for the different protein solutions at  $20 \text{ }^\circ\text{C}$  from  
 259 shear rate of 1 - **1000** at  $20 \text{ }^\circ\text{C}$ .

Protein isolate	Conc. (%)	K	n	( $R^2$ )	$\mu_{\text{ap}}$ (mPa.s) at $100 \text{ s}^{-1}$
Soy protein	12	25424	0.32	0.98	$1124.26 \pm 110.98$
	10	2542.5	0.39	0.99	$59.26 \pm 8.41$
	7	410.52	0.55	0.99	$15.44 \pm 0.35$
	5	68.001	0.69	0.98	$6.36 \pm 0.09$
	4	32.993	0.74	0.9158	$4.16 \pm 0.06$
Pea protein	12	1871.10	0.56	0.99	$228.425 \pm 4.35$
	10	299.50	0.67	0.96	$126.62 \pm 11.31$
	7	64.19	0.72	0.93	$39.475 \pm 1.43$
	5	17.74	0.82	0.84	$14 \pm 0.50$
	4	9.92	0.80	0.87	$8.15 \pm 4.03$
Faba bean	12	362.74	0.69	0.99	$79.20 \pm 10.32$
	10	66.99	0.64	0.85	$10.10 \pm 0.30$
	7	9.40	0.98	0.11	$7.89 \pm 0.15$

260 *The coefficient of determination ( $R^2$ ) was obtained from experimental data. Values of apparent*  
 261 *viscosity are reported as mean  $\pm$  standard deviation ( $n = 4$ ). Values of viscosity at  $100 \text{ s}^{-1}$  were*  
 262 *obtained from the experimental data.*

263

264 These parameters exhibited trends consistent with those observed in the viscosity curves. All  
 265 proteins demonstrated a concentration-dependent decrease in the power law index. Typically,  
 266 greater shear thinning is observed at higher polymer concentrations due to increased polymer



267 entanglement, which correlates with higher viscosity (Wittek et al., 2020). Shear thinning  
268 behaviour in globular plant proteins involves a marked reduction in the viscosity of a protein  
269 suspension as the shear rate increases. This phenomenon occurs because applied shear stress  
270 disrupts protein-protein interactions and promotes the alignment of protein molecules within  
271 the suspension. The globular shape of these proteins facilitates their reorientation and mobility  
272 under shear, contributing to the observed decrease in viscosity (Liang et al., 2016; McClements,  
273 2023). Overall, increasing protein concentration led to an increase in  $K$  (consistency  
274 coefficient) and a corresponding decrease in  $n$  (power law index). The power-law parameters  
275 were derived by fitting the data from shear rates of 1 to 1000  $\text{s}^{-1}$ , as depicted in the viscosity  
276 curves (log-log plot shown in **Fig. 1**). As protein concentration increased from 4 % to 12 %,  
277 the exponent  $n$  decreased from 0.74 to 0.32, approaching zero in the case of soy protein. A  
278 similar trend was observed for pea and faba bean proteins. At higher protein concentrations (12  
279 % protein basis), the exponent  $n$  approached zero for soy ( $n = 0.32$ ) and pea ( $n = 0.56$ ), whereas  
280 it remained higher for faba bean protein ( $n = 0.69$ ). As protein concentration decreases, so does  
281 the viscosity, as protein content is the primary determinant of the system's viscosity.  
282 Understanding the viscosity behaviour of protein suspensions is crucial for industrial  
283 applications, as it influences the design and optimization of various unit operations and  
284 processes in food product development.

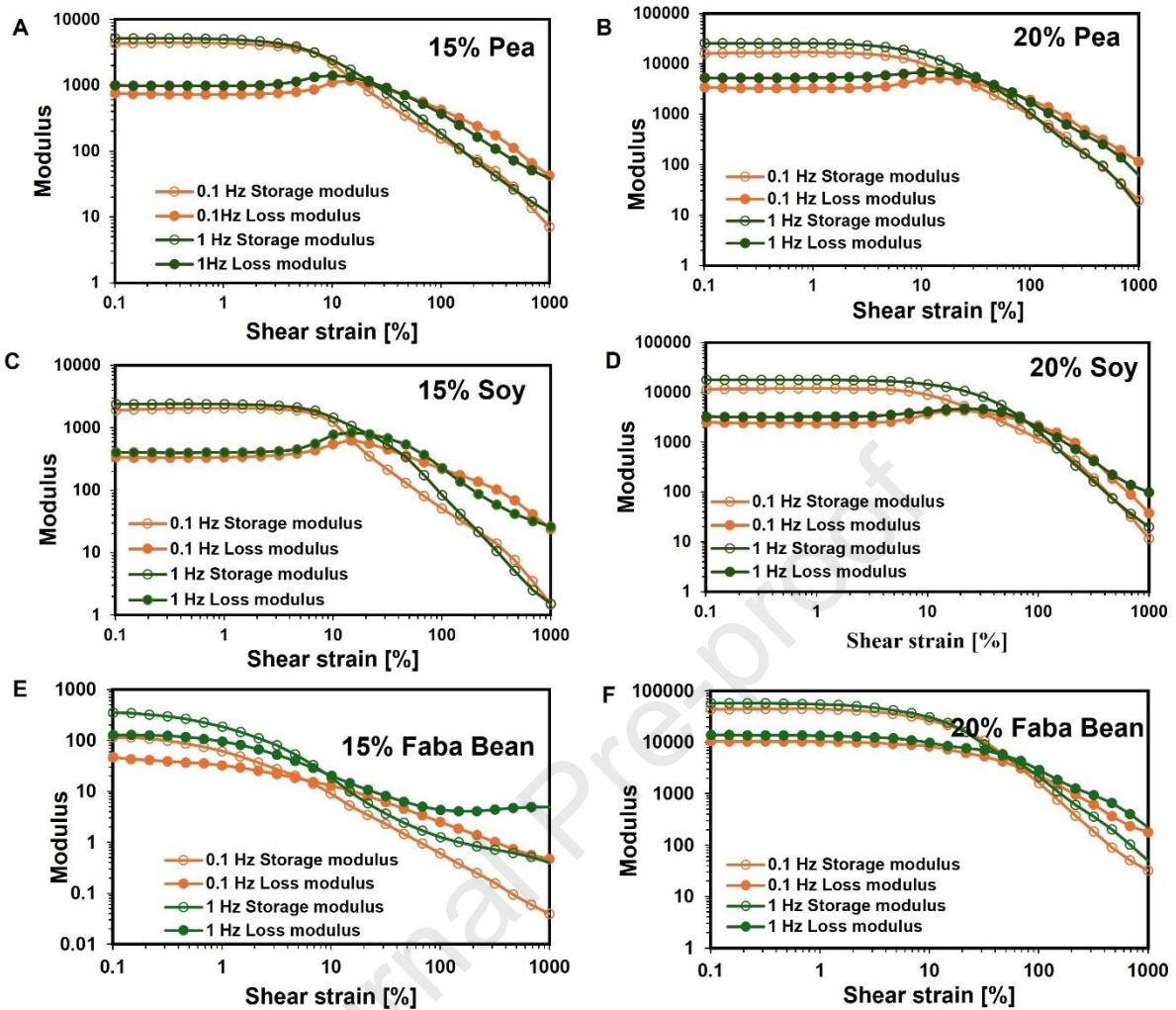
285

### 286 **Amplitude sweeps of Protein dispersion**

287 Viscoelastic materials can be categorized as either viscoelastic solids or liquids based on their  
288 response to applied stress. When stress is applied to a viscoelastic solid, it deforms at a finite  
289 rate until it reaches a fixed deformation, and upon removal of the stress, it gradually returns to  
290 its original dimensions. In contrast, a viscoelastic liquid continues to flow as long as the stress

291 is applied and only partially recovers its original shape once the stress is removed. The  
292 rheological properties of viscoelastic materials are typically assessed by measuring their  
293 dynamic shear rheology ( $G$ ) as a function of time, frequency, strain, or temperature. Amplitude  
294 sweep tests were conducted over a range of strains to evaluate both the linear viscoelastic (LVE)  
295 and non-linear viscoelastic (non-LVE) behaviour of these protein suspensions (McClements,  
296 2023; Wittek et al., 2020).

297 The findings indicate that at low strain values, the biopolymer suspensions demonstrate linear  
298 viscoelastic (LVE) behaviour, characterized by constant plateau values for both the storage  
299 modulus ( $G'$ ) and the loss modulus ( $G''$ ) within the low deformation range. As the strain  
300 exceeds the LVE regime, these protein suspensions exhibit a yield point and a cross-over point.  
301 The study observed at protein concentration of 15 and 20 % that both the storage and loss  
302 moduli remained relatively stable at low applied strains ( $< LVR$ ) but decreased significantly  
303 when the strain exceeded approximately 1 % (**Fig 2**). Typically, the storage modulus ( $G'$ ) was  
304 higher than the loss modulus ( $G''$ ) across the strain range of 0.1 to 10 %, except at a 12 %  
305 protein concentration for soy and US-FBP (data not shown). Generally, the modulus values  
306 were higher at 1 Hz compared to those at 0.1 Hz. At a 12 % protein concentration, soy protein  
307 exhibited the highest moduli, followed by US-FB protein, with pea protein showing the lowest.  
308 For the 15 % protein solution, pea protein displayed the highest moduli compared to soy and  
309 US-FBP protein. The critical yield strain at 12 % protein concentration was found to be less  
310 than 1%.



311

312

313 **Fig. 2.** Amplitude sweep test of **15 and 20 % wt.** protein suspension results demonstrate how  
 314 the dynamic storage modulus ( $G'$ ) and loss modulus ( $G''$ ) vary with shear strain ( $\gamma$ ) at constant  
 315 frequencies of 0.1 Hz and 1 Hz at 20 °C.

316 The yield strain values were approximately 1.48 % for pea protein, 3.18 % for soy protein, and  
 317 0.2 % for US-FBP at a concentration of 15%. A similar trend was observed at 20 % protein  
 318 concentration, with yield strains increasing as the protein concentration rose. Specifically, at  
 319 20 %, the yield strain for pea protein was 2.17 %, for soy protein was 4.67 %, and for US-FBP  
 320 was **1.01** %. The cross-over strain was found to be greater than 10 % for all samples at both 15  
 321 % and 20 % protein concentrations. The dynamic storage modulus ( $G'$ ) and loss modulus ( $G''$ )  
 322 of the protein dispersions increased significantly with higher protein concentrations. The

323 constant plateau values at low strains suggest that these protein solutions behave predominantly  
324 as solid-like materials within this strain range. At higher deformation amplitudes, the  $G'$  values  
325 decrease due to the disruption of the protein structure. The cross-over between  $G'$  and  $G''$   
326 indicates a transition from solid-like to liquid-like behaviour.

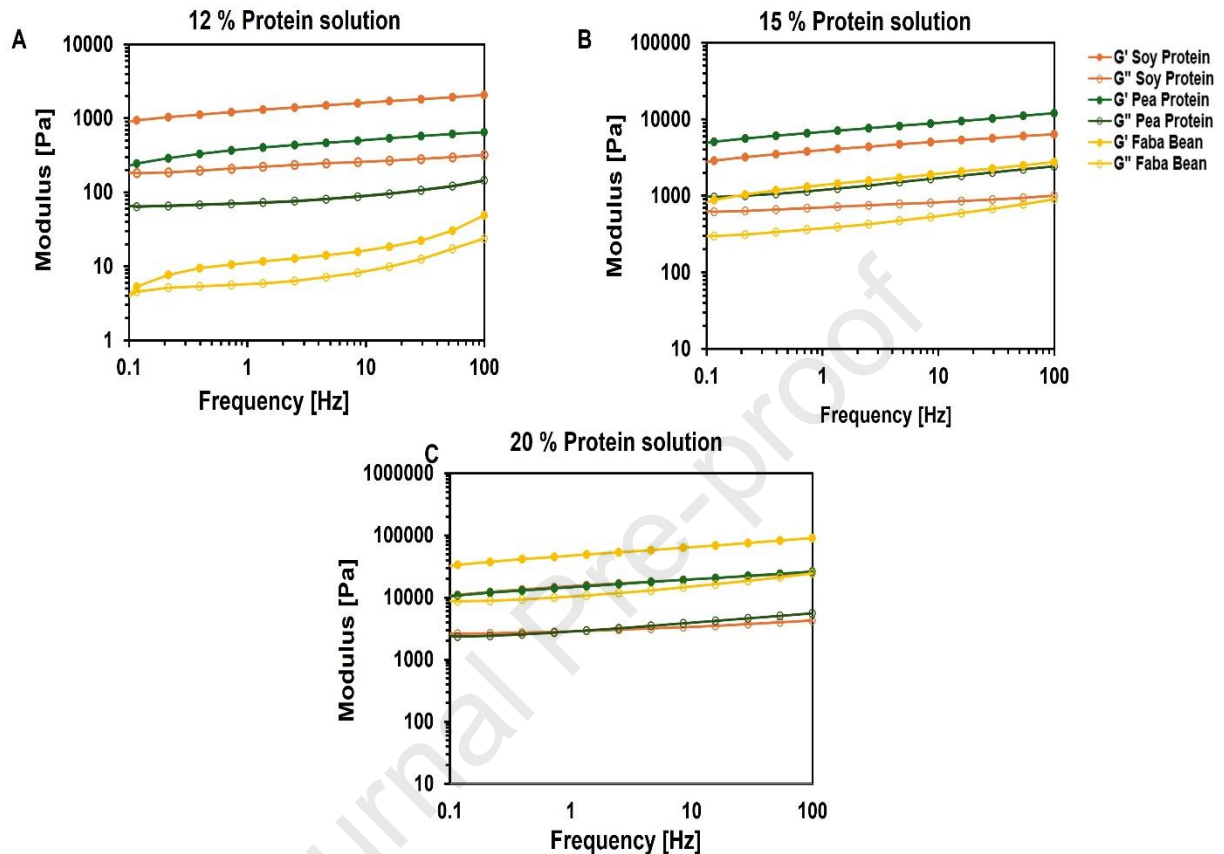
327

### 328 **Frequency sweep**

329 Conducting both small-amplitude oscillatory shear (SAOS) and large-amplitude oscillatory  
330 shear (LAOS) experiments on protein suspensions with concentrations ranging from 12 to 20  
331 % w/v allows for reliable identification and quantification of structural changes occurring  
332 during aggregation and breakdown, as well as approximation of processing-induced structural  
333 transformations. Rheological measurements of textural attributes in solid or semi-solid foods  
334 can provide valuable insights when changes in their properties are assessed in response to  
335 varying frequencies of applied oscillatory shear stress (Okeudo-Cogan et al., 2023). Frequency  
336 sweep tests, conducted over an angular frequency range of 0.1 to 100 Hz with a constant strain  
337 amplitude of 0.2 %, assess the stability of protein suspensions within this frequency range  
338 (**Fig.3**). The amplitude sweep test confirmed that 0.2 % strain falls within the linear viscoelastic  
339 (LVE) region for all samples studied. Thus, frequency sweep tests offer insights into the

340 stability of the protein suspensions at this constant strain amplitude across the measured  
 341 frequency range.

342



343 **Fig.3.** The frequency sweep tests illustrate the changes in the dynamic storage modulus ( $G'$ )  
 344 and loss modulus ( $G''$ ) as a function of shear frequency for various protein suspensions, with a  
 345 constant strain of 0.2 %.

346

347 The viscoelastic properties, represented by the dynamic storage modulus ( $G'$ ) and loss modulus  
 348 ( $G''$ ), were plotted against oscillation frequency to assess how the yielding region evolves with  
 349 increasing concentration (**Fig. 3**). At concentrations ranging from 12 to 20 %, the storage  
 350 modulus consistently exceeded the loss modulus across the entire frequency spectrum,  
 351 indicating that the protein suspensions predominantly exhibited elastic behaviour. A slight  
 352 increase in both moduli was observed with increased frequency, likely due to the structural  
 353 components of the proteins having less time to react to the oscillating stress at higher

354 frequencies, resulting in greater resistance to deformation. At 12 % concentration, soy protein  
355 demonstrated the highest  $G'$ , followed by pea protein, with US-faba bean protein showing the  
356 lowest. On the contrary, at 20 % concentration, US-faba bean protein exhibited the highest  $G'$ ,  
357 followed by soy and pea proteins. We hypothesize that the observed improvement in  $G'$  of US-  
358 FBP can be attributed to several factors. First, the high protein purity in US-FBP compared to  
359 soy and pea proteins likely reduced the influence of starch and fibres at lower protein  
360 concentrations (12 and 15 %), minimizing the "filler effect." Previous studies have indicated  
361 that even small amounts of starch can enhance the number of linkages within protein networks  
362 (Lyu et al., 2022). At a protein concentration of 20 %, the increased solid volume fraction may  
363 have contributed to the elevated  $G'$ . Additionally, the shear modulus of a suspension is  
364 influenced by the volume fraction of dispersed particles ( $\phi$ ), as described by the Eilers and Dijk  
365 equation, which links shear modulus to  $\phi$  and introduces a maximum packing fraction ( $\phi_m$ ) for  
366 concentrated suspensions (Ferry, 1980). The  $\phi_m$  value depends on particle size distribution and  
367 interparticle interactions. Therefore, we propose that enhanced protein-protein interactions,  
368 surpassing protein-water interactions, resulted in a denser, interconnected protein matrix at 20  
369 % protein concentration, leading to higher shear modulus behaviour in US-FBP.

### 370 **Least gelation capacity**

371 The gelation behaviour of protein solutions was assessed by examining the least gelling  
372 concentration and rheological properties, as these factors are influenced by both molecular and  
373 colloidal interactions. The results for least gelling concentration were confirmed by both  
374 observation and strain sweep measurement are shown in **Table 4**. A gel was considered a weak  
375 gel if the gel was semi-solid while strong gels was considered self-supporting upon inversion.  
376 At a neutral pH of 7, a concentration of 10 % w/v was sufficient to form a self-standing gel for  
377 pea, soy, and ultrasound-extracted faba bean protein isolates. In contrast, a higher concentration  
378 of 12 % w/v was needed for whey protein to achieve gel formation. For soy protein isolate,

379 concentrations of 15 and 20 % w/v produced strong gels; however, these gels exhibited  
 380 breakage and slipping when inverted as shown in **Fig.4**.

381

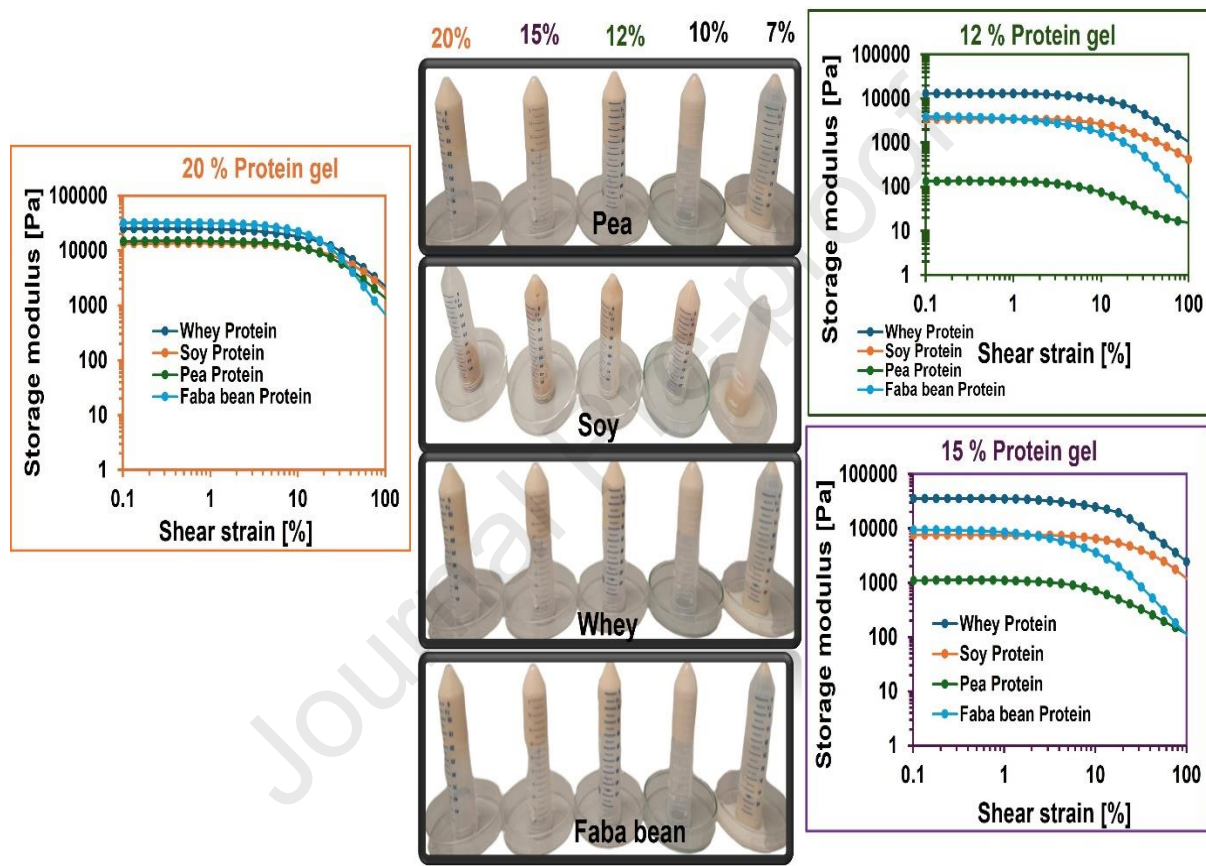
382 **Table 4:** Mapping of least gelation concentration of commercial plant-based protein isolates  
 383 gels (heating at 90 °C for 1 hr followed by cooling at 4 °C for 12 hr).

Concentration (%)	Pea Isolate	Soy Isolate	U-Faba bean Isolate	Whey Protein
2	X	X	X	X
4	X	X	X	X
5	X	X	X	X
7	X	X	X	X
10	✓	✓	✓	▲
12	✓	✓	✓	✓
15	✓	✓	✓	✓
20	✓	✓	✓	✓

384 X no gel, ▲ weak gel, ✓ strong gel.

385 Strain sweep tests conducted over a broad strain range (0.1–100 s<sup>-1</sup>) after heat-induced gelation  
 386 revealed differences in the viscoelastic properties of the heat-set gels. Gels prepared with  
 387 protein concentrations at 12 to 20 % exhibited a typical viscoelastic gel-like structure,  
 388 characterized by G' exceeding G'' throughout the strain range (Fig. 4) indicating the dominance  
 389 of elastic properties. Notably, the rheological properties of the gels varied depending on the  
 390 type of protein used. For 12% heat-set gels, whey protein displayed the highest G', followed  
 391 by soy and ultrasound-extracted faba bean proteins, with pea protein showing the lowest G'.  
 392 As anticipated, increasing the protein concentration for all proteins to 15 and 20 % led to a  
 393 noticeable increase in G' for **all the studied proteins**. **All gels** at 12% protein concentration

394 exhibited a yield strain of approximately 1.35 %, which increased to ~2.5 % at 15 %  
 395 concentration (**Fig.4**). The higher yield strains observed in soy and US-FBP gels compared to  
 396 pea protein are consistent with findings reported in the literature (Hua et al., 2005; Shand et al.,  
 397 2007).  
 398



399 **Fig. 4.** Least gelation concentration with an associated strain sweep of heat set gels (heating at  
 400 90 °C for 1 hr followed by cooling at 4 °C for 12 hr). Strain sweep was performed after gel  
 401 formation.

402

403 The observed differences in gelation properties between soy protein isolate (SPI) and pea  
 404 protein isolate (PPI) can be attributed to the distinct compositions of their globulin fractions.  
 405 Soybean globulins, predominantly glycinin (11S) and  $\beta$ -conglycinin (7S), exhibit higher  
 406 solubility compared to pea globulins, which are mainly legumin (11S) and vicilin (7S). At a



407 higher protein concentration of 20 % w/v, US-FBP demonstrated a  $G'$  comparable to that of  
408 whey protein, whereas soy and pea proteins exhibited lower  $G'$  values. All heat-set gels at 20  
409 % protein concentration displayed a similar yield strain of approximately 5%. For all protein  
410 types, the  $G'$  was greater than  $G''$ , indicating successful gel formation. The gelation behaviour  
411 of plant proteins is influenced by multiple factors, including protein concentration, type,  
412 extraction and processing conditions, and the presence of other components such as starch,  
413 complex carbohydrates (fibres), and salts (Ma, Greis, et al., 2022b; Tanger et al., 2021).  
414 Compositional differences among protein sources, such as varying levels of salts, fibers, and  
415 starch, can significantly impact and interfere with gelation. Proteins are primarily regarded as  
416 matrix formers when adequately hydrated, whereas other biopolymers, particularly complex  
417 polysaccharides found in unrefined ingredients like soy and pea, act as fillers, enhancing water  
418 retention within the matrix and influencing gel strength (van der Sman & van der Goot, 2023).  
419 Starch also plays a role in structure formation due to its water-binding capacity, which can  
420 modify gel strength depending on the starch type. During thermal processing, starch undergoes  
421 volume changes through swelling, gelling, degradation, and setting, further affecting gel  
422 characteristics (Bühler et al., 2022). High levels of fibres and starch in pea and soy proteins  
423 may partially entrap proteins within cellular matrices, reducing their availability for effective  
424 gel formation. In contrast, the high protein purity of US-FBP likely minimizes the presence of  
425 fibres and starch, reducing competition for water and facilitating the formation of stronger  
426 protein gel networks.

427

428

429

430

**431 In situ gelation (Temperature sweep)**

432 Small amplitude oscillatory measurements examine the dynamic rheological properties without  
433 disturbing the internal network structure. Strain amplitudes in this range are too small to disrupt  
434 the gel microstructure, ensuring that the mechanical responses of gels in the linear viscoelastic  
435 (LVE) region remain unaffected by the applied stress or strain (Xia et al., 2022). For  
436 viscoelastic property measurements, an oscillatory strain of 0.2 % within the LVE range was  
437 used. During heat-induced gelation, the protein dispersions transitioned from a viscous liquid  
438 to a semi-solid, and eventually to a gel-like structure. The viscoelastic properties, specifically  
439 the storage modulus ( $G'$ ) and loss modulus ( $G''$ ), of the various protein dispersions (12 and  
440 15%) were monitored as a function of temperature (heating from 20 to 90 °C and cooled to 20  
441 °C). The heat-induced gelation process involved a cycle of heating, holding, and cooling  
442 (**Fig.5.A**). In viscoelastic materials, the storage modulus ( $G'$ ) and loss modulus ( $G''$ ) represent  
443 the elastic (non-dissipative) and viscous (dissipative) components, respectively (Mohamed et  
444 al., 2009). At all protein concentrations, US-FBP gels exhibited the highest  $G'$  compared to pea  
445 and soy proteins. This indicates that US-FBP shows strong potential for use in meat analogue  
446 development through extrusion, even with high moisture content. This is due to its ability to  
447 form stronger gels at lower concentrations and temperatures (Xia et al., 2021). Among all the  
448 plant proteins studied, pea protein had the lowest  $G'$  at both the beginning and end of the heating  
449 process, confirming the superior gelation behaviour of faba bean and soy protein isolates  
450 compared to pea protein isolates (Shrestha et al., 2023). The differences in gel strength among  
451 the studied proteins can be attributed to several factors previously discussed. One key factor is  
452 the presence of constituents such as fibres and starch, which can modulate and interfere with  
453 the formation of robust protein gels. In pea and soy proteins, the high levels of starch and fibres,  
454 along with the diverse side groups present in these components, may lead to intramolecular  
455 interactions, cross-linking, and entanglement during gelation, potentially hindering the

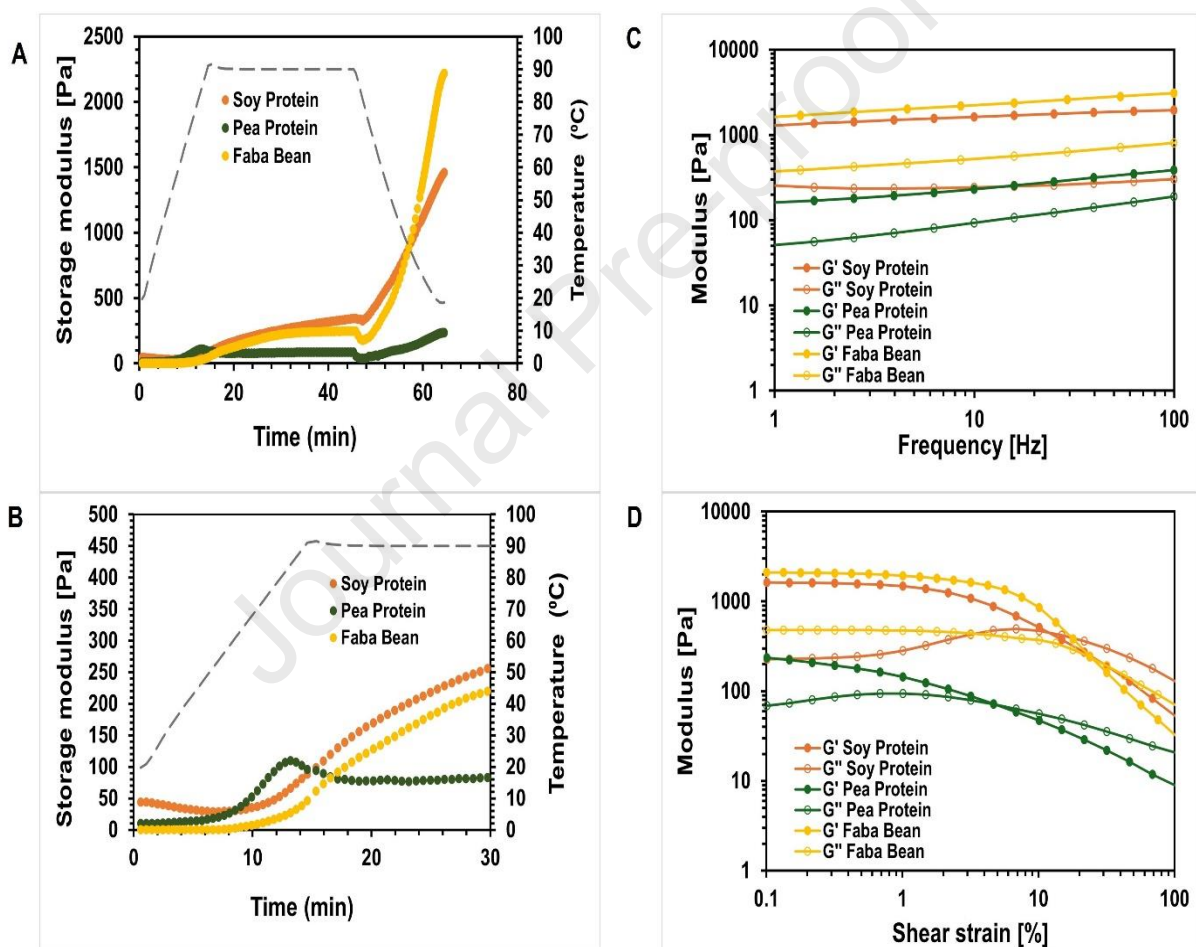
456 development of strong gels. Furthermore, the intrinsic properties of the protein types, such as  
457 differences in secondary structure and solubility, contribute to the distinct gelation behaviours  
458 observed for soy, pea, and faba bean proteins (Bora et al., 1994; Johansson et al., 2023).

459 Within the temperature range of 20 – 50 °C (**Fig.5.B**), the storage modulus ( $G'$ ) of US-FBP  
460 started lower than that of soy and pea proteins but gradually increased, surpassing pea protein  
461 as the temperature rose. This increase suggests that thermal softening in faba bean protein was  
462 likely offset by an increase in bond density, with a notable rise in  $G'$  occurring between 50 and  
463 65 °C and an inflection point around 45 °C, indicating enhanced physical crosslinking  
464 dynamics that strengthen the network. For pea protein gels, network formation mainly relies  
465 on physical bonds such as hydrogen bonding and hydrophobic interactions between protein  
466 molecules (Sun & Arntfield, 2012) , which intensify when proteins unfold due to heating. Pea  
467 protein formed spherical and hollow aggregates and particles, and heating above approximately  
468 50 °C caused a steep increase in shear modulus due to protein unfolding and aggregation around  
469 the thermal denaturation temperature, forming a 3D elastic network. A similar observation was  
470 made for US-FBP and soy protein, where gel network formation in faba bean protein has been  
471 attributed to the exposure of initially buried hydrophobic groups during heating (Hall &  
472 Moraru, 2021). The gelation process is thought to proceed through several mechanisms: (1)  
473 protein denaturation, (2) formation of crosslinks between denatured proteins, (3) aggregate  
474 formation from these crosslinked proteins, and (4) continued aggregate growth leading to gel  
475 formation (Clark et al., 2001). In less refined proteins such as soy and pea, the presence of  
476 components like fibres and starch can alter this gelation process, resulting in diverse gel  
477 structures. This is because the polarity and charge of biopolymers affect their interactions,  
478 including hydrophobic, hydrogen bonding, and electrostatic interactions, which are determined  
479 by the number of non-polar, polar, and charged groups in the biopolymer chains (McClements,

480 2023). These interactions significantly influence the structuring and gelling behaviour of the  
 481 proteins.

482 Further heating caused a slight increase in shear modulus as more protein molecules unfolded  
 483 and joined the network. Upon cooling from 90 to 20 °C, there was a significant increase in  
 484 shear modulus, attributed to the strengthening of hydrogen bonds between protein molecules  
 485 in the gel network.

486



487

488 **Fig. 5.** (A) Temperature sweep (20 – 90 – 20 °C,  $f = 1$  Hz,  $\gamma = 0.2$  %) of gels formed at 12 %  
 489 protein dispersion with temperature represented by dash line; (B) heating part of the  
 490 temperature sweep (20 – 90 °C); (C) frequency sweep; and (D) strain sweep at 20 °C.  $G'$  is  
 491 indicated by filled symbols, and  $G''$  empty symbols.

492 The effect of heating and cooling on 15 % protein dispersions of the three plant proteins is  
493 shown in **Fig.6. A**. The storage profile of 15 % dispersions of pea and soy proteins differed  
494 from the 12% storage profile. As observed in previous studies, the initial heating of 15 % pea  
495 and soy protein gels during the first 30 minutes (**Fig.6.B**) temporarily weakened the gels, but  
496 subsequent cooling restored their original strength, indicating the reformation of attractive  
497 forces between protein aggregates. Additionally, for proteins rich in thiol groups, the moduli  
498 can increase over time as the gel structure cools completely, due to the formation of disulfide  
499 bridges (Alting et al., 2003). However, for 15 % US-FBP, a similar trend to the 12 % gels was  
500 observed, with improved moduli. At the end of the cooling cycle for all 12 % protein gels, the  
501 values of  $G'$ ,  $G''$ , and the loss factor were recorded to assess the gel strength of the proteins as  
502 shown in **Table 5**. Whey proteins exhibited the highest  $G'$  at  $2.48E+04$  and the lowest loss  
503 factor of 0.17, indicating the formation of a very strong gel compared to plant-based proteins.  
504 Among the plant proteins, ultrasound-extracted faba bean (US-FBP) had the highest  $G'$  of 2218  
505 Pa with a loss factor of 0.24, while soy protein had a  $G'$  of 1458 Pa and a loss factor of 0.19.  
506 Based on the loss factor, soy protein formed a relatively stronger gel than U-faba bean. Pea  
507 protein exhibited the lowest  $G'$  at 236.27 Pa and a high loss factor of 0.373, indicating a weaker  
508 gel compared to soy and U-faba bean. For the 15 % gels, an increase in both  $G'$  and  $G''$  was  
509 observed at the end of the cooling cycle for all proteins. US-FBP showed the highest  $G'$   
510 (**6037.55 Pa**) compared to soy (3107.8 Pa) and pea (2306.7 Pa) (**Table 5**). All the 15 % heat-  
511 set gels demonstrated a strong gel characteristic based on their loss factors (ranging from 0.18  
512 to 0.22).

513

514

515

516 **Table 5.** Measured  $G'$ ,  $G''$  and  $\tan\delta$  of heat induced gels at the end of the cooling cycle for  
 517 different proteins suspensions (12 and 15 %).

518

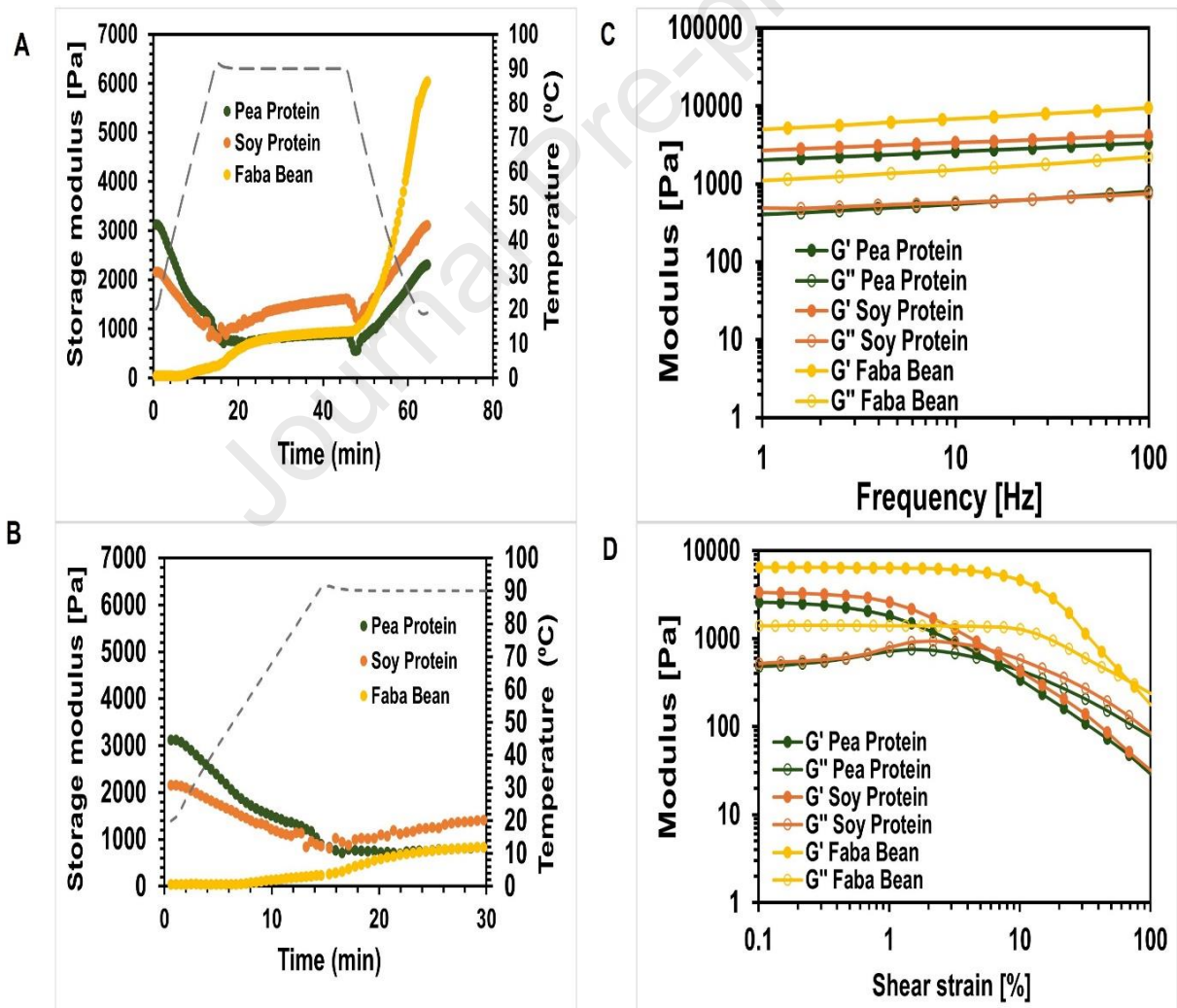
Samples	$G'$ (Pa)	$G''$ (Pa)	loss factor ( $\tan\delta$ )	Aspect
Soy Protein (12%)	$1458.45 \pm 60.74$	$274.60 \pm$ 10.09	$0.19 \pm 0.02$	Strong Gel
Soy Protein (15%)	$3107.8 \pm 431.06$	$541.94 \pm$ 58.24	$0.18 \pm 0.01$	Strong Gel
Pea Protein (12%)	$236.27 \pm 29.51$	$87.57 \pm 0.32$	$0.37 \pm 0.05$	Weak Gel
Pea Protein (15%)	$2306.7 \pm 625.51$	$504.05 \pm$ 107.33	$0.22 \pm 0.01$	Strong Gel
Faba bean protein (12%)	$2218.05 \pm 431.69$	$540.07 \pm$ 108.33	$0.24 \pm 0.00$	Strong Gel
Faba bean protein (15%)	6037.55 $\pm 2375.81$	1373.28 $\pm 547.62$	$0.23 \pm 0.00$	Strong Gel
Whey Protein (12%)	$2.48E+04 \pm 1448.16$	$4086.15 \pm$ 272.17	$0.17 \pm 0.00$	Very strong Gel

519

520 After completing the heating and cooling cycle, a frequency sweep (at a constant strain of 0.2  
 521 %) and an amplitude sweep (at a constant frequency of 1 Hz) were performed to further  
 522 characterize the rheological properties of the gels, including their non-linear viscoelastic  
 523 properties up to gel rupture. The gels exhibited distinct behaviours in the amplitude sweep (**Fig.**  
 524 **5.D & 6. D**): they displayed a clear linear viscoelastic (LVE) regime at low strain. Beyond this

525 regime, both  $G'$  and  $G''$  decreased due to the large shear strain causing partial rupture of the  
 526 network bonds that stabilize the gel structure. From the amplitude test, two parameters were  
 527 derived: the critical strain ( $\gamma_c$ ) and the crossover strain ( $\gamma_{G' = G''}$ ), along with the loss factor.  
 528 The critical strain was defined as the shear strain at the end of the LVE regime, where the  
 529 measured  $G'$  value deviated by 5 % from the initial  $G'$  value (Schlangen et al., 2022b). Beyond  
 530 this point, the initial gel structure begins to break down. The crossover strain was defined as  
 531 the point where the measured  $G'$  value was last higher than the  $G''$  value. These parameters  
 532 together indicate the gel's ability to withstand deformation.

533



534

535 **Fig. 6.** (A) Temperature sweep (20 – 90 – 20 °C,  $f = 1$  Hz,  $\gamma = 0.2\%$ ) of gels formed at 15 %  
 536 protein dispersion, Temperature: dash line; (B) heating part of the temperature sweep (20–90 °  
 537 C); (C) frequency sweep and (D) strain sweep at 20 °C.  $G'$ : filled symbols;  $G''$ : empty symbols.

538 Focusing on the  $\gamma_c$  values (**Table 6**), whey protein gel showed the highest value of 3.18 %,  
 539 indicating it can withstand significant deformation before rupturing. For 12% protein gels, the  
 540 lowest critical strain was observed for pea protein ( $\gamma_c = 0.10$  %), followed by soy (0.47 %),  
 541 with US-FBP exhibiting the highest  $\gamma_c$  (1.34 %). A lower  $\gamma_c$  value indicated that pea and soy  
 542 gels were easier to disrupt compared to US-FBP. Similar trends were observed for 15 % heat-  
 543 set gels, with faba bean dispersion showing an improved critical strain (3.18 %) (**Table 6**). In  
 544 combination with the  $\gamma_c$  results, materials with lower  $\gamma_c$  and  $\gamma_{G'=G''}$  values had a more brittle  
 545 texture and yielded sooner. When focusing on  $\gamma_{G'=G''}$ , US-FBP displayed a higher value (23.8  
 546 %) compared to soy (14.8%) and pea (4.67 %). Again, for 15 % dispersion, US-faba bean  
 547 protein showed the highest  $\gamma_{G'=G''}$  in comparison to pea and soy proteins. In combination  
 548 with the  $\gamma_c$  results, one can interpret those materials with lower  $\gamma_c$  and  $\gamma_{G'=G''}$  values had  
 549 more brittle texture that yielded sooner. When focusing on  $\gamma_{G'=G''}$ , US-FBPf showed a higher  
 550 value (23.8 %) compared to soy (14.8) and pea (4.67 %).

551 **Table 6.** Comparison of  $G'$ ,  $\tan \delta$ ,  $\gamma_c$  and  $\gamma_{G'=G''}$  after performing strain sweep of 12 and 15  
 552 % heat induced gels.

Samples	$G'$ (Pa)	$\tan \delta$	$\gamma_c$ (%)	$\gamma_{G'=G''}$ (%)
Soy Protein (12%)	1537.65 ± 48.44	0.17 ± 0.00	0.47	14.8
Soy Protein (15%)	3405.9 ± 346	0.15 ± 0.01	0.47	15.30
Pea Protein (12%)	236.025 ± 30.24	0.28 ± 0.02	0.10	4.67
Pea Protein (15%)	2660.7 ± 679	0.17 ± 0.00	0.10	6.85



Faba Bean (12%)	1880.55 ± 270.61	0.25 ± 0.0	1.34	23.8
Faba Bean (15%)	6053.75 ± 2183	0.23 ± 0.00	3.18	75.4
Whey Protein (12%)	21476 ± 1513.21	0.17 ± 0.00	3.18	217

553

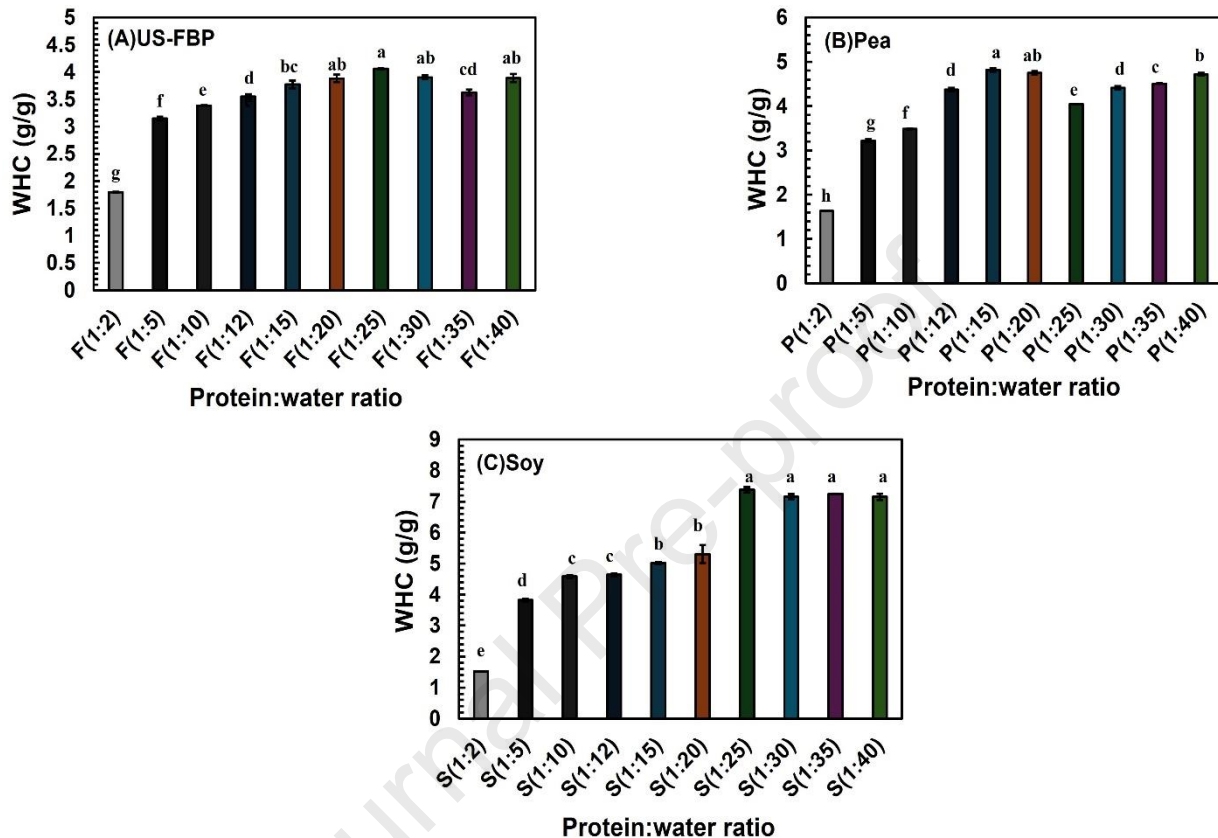
554 In the frequency sweeps (**Fig.5.B & 6.B**), the gels exhibited similar weak frequency  
 555 dependence, indicating gel networks with very broad spectra of relaxation times (Ren et al.,  
 556 2024). Additionally, the storage modulus ( $G'$ ) of all protein gels was significantly higher than  
 557 the loss modulus ( $G''$ ) within the tested frequency range, confirming that the heat-set gels were  
 558 predominantly elastic. This trend was also observed for the 15 % gelled proteins, which showed  
 559 increased moduli. Both  $G'$  and  $G''$  of all the gels slightly increased with increasing frequency,  
 560 with pea protein exhibiting the highest increase compared to soy and U-faba bean.

### 561 **Water holding capacity**

562 Water holding capacity ( $WHC$ ) can serve as an indicator of protein state and functionality. The  
 563 interaction of proteins with water is influenced by their amino acid composition and structure;  
 564 proteins that hold more water tend to have higher levels of exposed hydrophilic groups and  
 565 more charged amino acids (Ma, Grossmann, et al., 2022). As shown in **Fig. 7**, the  $WHC$  values  
 566 for the three proteins varied significantly from protein/water ratio of 1:2 to 1:40. For all  
 567 samples,  $WHC$  values increased with higher water addition, except at higher concentrations.  
 568 The mean  $WHC$  for soy protein ranged from 1.52 to 7.38 g/g (**Fig.7.C**). A reduction in  $WHC$   
 569 was observed beyond a solute/solvent ratio of 1:25 g/mL, with no significant difference ( $p <$   
 570 0.05) between ratios of 1:25 to 1:40 g/mL. Pea protein showed similar trends with some  
 571 variations. The  $WHC$  of pea protein ranged from 1.64 to 4.75 g/g (**Fig.7.B.**), which was lower  
 572 than that of soy protein.  $WHC$  increased from 1:2 to 1:20 g/mL, followed by a decrease from

573 1:25 to 1:35 g/mL. Significant differences ( $p < 0.05$ ) in WHC were observed for pea protein at  
 574 different solute/solvent ratios.

575



576

577 **Fig. 7.** Water holding capacity of (A) Faba bean protein isolate; (B) Pea protein and (C) Soy  
 578 protein at different protein to water ratios. Values are reported as mean  $\pm$  standard deviation ( $n$   
 579 = 3). The different letters denote significant differences ( $P < 0.05$ ) between samples.

580 The *WHC* of US-FBP ranged from 1.80 to 4.06 g/g, with the highest value (4.06 g/g) observed  
 581 at a solute/solvent ratio of 1:25 g/mL. Significant differences ( $p < 0.05$ ) were noted for the  
 582 *WHC* of US-FBP across the different ratios ((**Fig.7. A.**)). At the 1:25 g/mL ratio, soy protein  
 583 exhibited the highest *WHC* (7.38 g/g), followed by US-FBP (4.06 g/g) and pea protein (4.05  
 584 g/g). The variations in *WHC* can be attributed to differences in extraction methods, ionic  
 585 strength, amino acid composition, hydrophobicity, and protein conformation (Ma, Greis, et al.,  
 586 2022a; Ma, Grossmann, et al., 2022). The slightly higher *WHC* of commercial soy protein

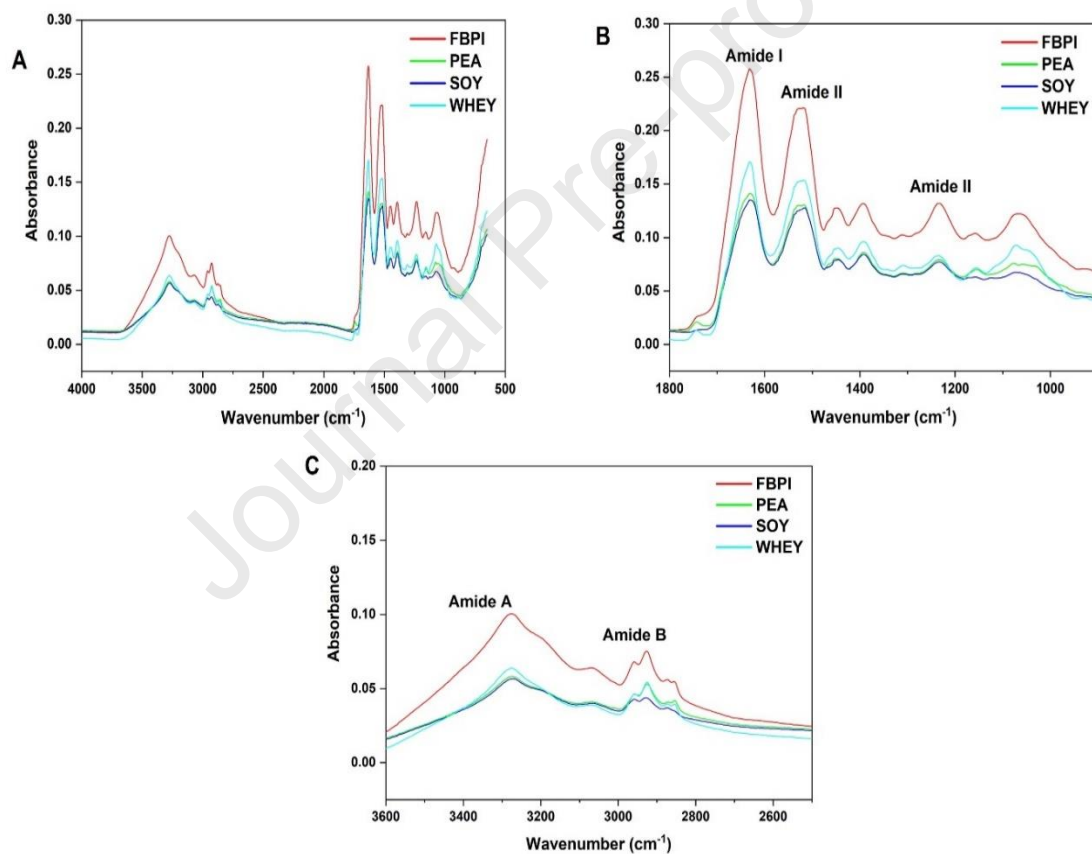
587 compared to laboratory-extracted faba bean protein likely relates to their structural unfolding  
588 (Osen et al., 2014), which exposes more hydrophobic amino acids. Complex polysaccharides  
589 (fibres) in less refined plant-based ingredients like soy and pea proteins are primarily described  
590 as fillers that contribute significantly to water-holding capacity (*WHC*) (van der Sman & van  
591 der Goot, 2023). Starch is also recognized for its strong water-binding properties. The high  
592 *WHC* of soy proteins has been attributed to protein subunits such as glycinin and  $\beta$ -conglycinin,  
593 which exhibit high water-binding capacity due to their elevated levels of polar amino acids  
594 (Schmid et al., 2024). Additionally, other components in soy protein, including starch, may  
595 further enhance its overall *WHC*. In contrast, the slightly lower *WHC* observed in pea protein  
596 compared to soy and US-FBP may result from higher levels of fiber and fat, which could  
597 negatively influence *WHC* (Farshi et al., 2024). It has been shown that depending on the type  
598 of fibre, starch and fat, *WHC* can be either negatively or positively impacted (Nagy et al., 2021).

#### 599 **Fourier Transform Infrared Spectroscopy (FTIR)**

600 ATR-FTIR is a technique frequently utilized to examine conformational differences among  
601 proteins (Tiernan et al., 2020). Analysis of the spectra reveals significant variations in  
602 absorption across the entire range of wavenumbers. Average spectra were obtained, displaying  
603 the characteristic band distribution of different plant protein isolates (**Fig. 8**). Pea and soy  
604 proteins exhibited the most similar overall spectra, while U-faba bean and whey proteins had  
605 distinct spectra. All protein samples showed major peaks in the Amide I, II, III, A, and B  
606 regions. Notable differences in intensity among the proteins were observed in the amide regions  
607 and the fingerprint region ( $1800 - 1200 \text{ cm}^{-1}$ ) between US-FBP compared to commercial  
608 proteins (soy and pea) (**Fig.8.B**). The Amide I region ( $1600\text{--}1700 \text{ cm}^{-1}$ ) is particularly  
609 significant due to its high conformational dependence and sensitivity. In contrast, the adjacent  
610 Amide II and III regions are less dependent on secondary structure content. The Amide I region  
611 primarily arises from C=O stretching vibrations and out-of-phase CN stretching vibrations of

612 the polypeptide backbone (Zhao et al., 2021). Each type of secondary structure contributes to  
613 absorption within a specific wavenumber range within the 1600–1700  $\text{cm}^{-1}$  region. Despite  
614 being commonly used due to its strong signal, the Amide I region (1700 -1600  $\text{cm}^{-1}$ ) has  
615 limitations, such as strong interference from water vibrational bands, relatively unstructured  
616 spectral contours, and overlap of bands corresponding to various secondary structures. This  
617 peak includes components such as  $\beta$ -sheets, random structures,  $\alpha$ -helix, and  $\beta$ -turns (Tiernan  
618 et al., 2020).

619



620

621 **Fig.8.** FTIR spectra of protein isolate powders of faba bean, pea, soy and whey protein; (a)  
622 original spectra; (b) Amide I - III region 1800 – 900  $\text{cm}^{-1}$  and (c) Amide A and B region 1200  
623 – 700  $\text{cm}^{-1}$ . Average of replicates (n=4).

624 Due to differences in protein content and presence of other constituents such as fibre and starch,  
625 spectral intensity variations were notably pronounced in the Amide I, II, and III regions. The  
626 average absorption magnitude of pea and soy proteins was lower compared to whey and US-  
627 FBP. The Amide III region is generally considered less sensitive in protein IR spectra, with its  
628 bands primarily arising from NH bending and CN stretching vibrations, which are  
629 conformationally dependent (Barth, 2007). Although the basic structural characteristics of the  
630 proteins remained constant for all the proteins, partial changes occurred in the band intensities.  
631 This differences in band intensity may be attributed to the composition and processing history  
632 of the final ingredient as commercial proteins (soy and pea) are usually produced using  
633 extensive conditions compared to laboratory extracted proteins (Ma, Greis, et al., 2022b;  
634 Nicolai & Chassenieux, 2019). As seen in **Fig.8.C**, the Amide A and B spectra effectively  
635 differentiate between the various protein samples. A major peak was observed around  $\sim 3300$   
636 and  $\sim 2900\text{ cm}^{-1}$ ; however, this peak was less pronounced in soy, pea, and whey proteins  
637 compared to U-faba bean protein, likely due to their comparatively lower protein content.

## 638 **Conclusion**

639 This study offers a comprehensive multi-scale experimental review of the primary viscoelastic  
640 and structural properties of promising plant proteins for potential use in the development of  
641 next-generation foods. The rheological, functional, structural, and thermal behaviours of  
642 commercial proteins (soy and pea) were compared to those of ultrasound-extracted faba bean  
643 protein (US-FBP). Based on viscosity measurements, the proteins ranked in order of viscosity  
644 as soy ( $n = 0.32$ ) > pea ( $0.56$ ) > US-FBP ( $0.69$ ), modelled by the power law and characterized  
645 by the consistency index ( $k$ ) and power law index ( $n$ ). Distinct gelling behaviours were  
646 observed among the plant proteins due to differences in molecular composition. The minimum  
647 gelation concentration was identified as 10 %, but gel strength varied, ranking U-faba bean >  
648 soy > pea. In situ gelation at 12 % showed a high  $G'$  for US-FBP ( $G' = 2218\text{ Pa}$ ) compared to

649 soy (1458 Pa) and Pea (236.27 Pa). Structural studies using FTIR analysis showed distinct  
650 spectra intensity difference in the protein regions was observed in the order of US-FBP < soy  
651 < pea protein. Among the proteins, US-faba bean protein exhibited the lowest water-holding  
652 capacity at various concentrations compared to the commercial proteins. In conclusion, this  
653 work provides valuable insights into tailoring plant proteins and tuning textural properties for  
654 developing sustainable food products.

655

656

657

#### 658 **Declaration of competing interest**

659 The authors declare that they have no known competing financial interests or personal  
660 relationships that could have appeared to influence the work reported in this paper.

#### 661 **Authorship contribution statement**

662 Conceptualization: Abraham Badjona, Bipro Dubey; methodology: Abraham Badjona,  
663 Beatrice Cheron, Bipro Dubey, Robert Bradshaw; Investigation: Abraham Badjona; Beatrice  
664 Cheron, Writing—original draft preparation: Abraham Badjona, Robert Bradshaw, Bipro  
665 Dubey; Project administration: Bipro Dubey, Robert Bradshaw and Abraham Badjona. All  
666 authors have read and agreed to the published version of the manuscript.

#### 667 **Acknowledgments**

668 The authors would like to thank Jonny Shepherd, and the NCEFE team at Sheffield Hallam  
669 University for the guidance received when performing the experiments.

#### 670 **Data Availability Statement**

671 The data generated during the current study are available upon reasonable request.

## 672 **Rights Retention Statement**

673 For the purpose of open access, the author has applied a Creative Commons Attribution  
674 (CCBY) licence to any Author Accepted Manuscript version of this paper arising from this  
675 submission.

676

677

678

679

680

681

682

683

684

685

686

687

## 688 **References**

689 Ansari, S., Rashid, M. A. I., Waghmare, P. R., & Nobes, D. S. (2020). Measurement of the flow  
690 behavior index of Newtonian and shear-thinning fluids via analysis of the flow velocity  
691 characteristics in a mini-channel. *SN Applied Sciences*, 2(11). [https://doi.org/10.1007/s42452-](https://doi.org/10.1007/s42452-020-03561-w)  
692 020-03561-w

- 693 Badjona, A., Bradshaw, R., Millman, C., Howarth, M., & Dubey, B. (2023). Faba Beans Protein as an  
694 Unconventional Protein Source for the Food Industry: Processing Influence on Nutritional,  
695 Techno-Functionality, and Bioactivity. In *Food Reviews International*. Taylor and Francis Ltd.  
696 <https://doi.org/10.1080/87559129.2023.2245036>
- 697 Badjona, A., Bradshaw, R., Millman, C., Howarth, M., & Dubey, B. (2024a). Optimization of  
698 ultrasound-assisted extraction of faba bean protein isolate: Structural, functional, and thermal  
699 properties. Part 2/2. *Ultrasonics Sonochemistry*, *110*, 107030.  
700 <https://doi.org/10.1016/j.ultsonch.2024.107030>
- 701 Badjona, A., Bradshaw, R., Millman, C., Howarth, M., & Dubey, B. (2024b). Response surface  
702 methodology guided approach for optimization of protein isolate from Faba bean. Part 1/2.  
703 *Ultrasonics Sonochemistry*, *109*, 107012. <https://doi.org/10.1016/j.ultsonch.2024.107012>
- 704 Badjona, A., Bradshaw, R., Millman, C., Howarth, M., & Dubey, B. (2024c). Structural, thermal, and  
705 physicochemical properties of ultrasound-assisted extraction of faba bean protein isolate (FPI).  
706 *Journal of Food Engineering*, *377*. <https://doi.org/10.1016/j.jfoodeng.2024.112082>
- 707 Barth, A. (2007). Infrared spectroscopy of proteins. In *Biochimica et Biophysica Acta - Bioenergetics*  
708 (Vol. 1767, Issue 9, pp. 1073–1101). <https://doi.org/10.1016/j.bbabi.2007.06.004>
- 709 Benoit, S. M., Afizah, M. N., Ruttarattanamongkol, K., & Rizvi, S. S. H. (2013). Effect of pH and  
710 temperature on the viscosity of texturized and commercial whey protein dispersions.  
711 *International Journal of Food Properties*, *16*(2), 322–330.  
712 <https://doi.org/10.1080/10942912.2011.552015>
- 713 Bora, P. S., Brekke, C. J., & Powers, J. R. (1994). *Heat Induced Gelation of Pea (Pisum sativum) Mixed*  
714 *Globulins, Vicilin and Legumin*.
- 715 Bühler, J. M., Schlangen, M., Möller, A. C., Bruins, M. E., & van der Goot, A. J. (2022). Starch in Plant-  
716 Based Meat Replacers: A New Approach to Using Endogenous Starch from Cereals and  
717 Legumes. In *Starch/Stärke* (Vol. 74, Issues 1–2). John Wiley and Sons Inc.  
718 <https://doi.org/10.1002/star.202100157>
- 719 Clark, A. H., Kavanagh, G. M., & Ross-Murphy, S. B. (2001). *Globular protein gelation: theory and*  
720 *experiment*. [www.elsevier.com/locate/foodhyd](http://www.elsevier.com/locate/foodhyd)
- 721 Coimbra, L., Costa, I. M., Evangelista, J. G., & Figueiredo, A. (2023). Food allergens in oral care  
722 products. *Scientific Reports*, *13*(1). <https://doi.org/10.1038/s41598-023-33125-y>
- 723 Farshi, P., Mirmohammadali, S. N., Rajpurohit, B., Smith, J. S., & Li, Y. (2024). Pea protein and starch:  
724 Functional properties and applications in edible films. *Journal of Agriculture and Food Research*,  
725 *15*. <https://doi.org/10.1016/j.jafr.2023.100927>
- 726 Ferry, J. D. . (1980). *Viscoelastic properties of polymers*. Wiley.
- 727 Hall, A. E., & Moraru, C. I. (2021). Structure and function of pea, lentil and faba bean proteins treated  
728 by high pressure processing and heat treatment. *LWT*, *152*.  
729 <https://doi.org/10.1016/j.lwt.2021.112349>
- 730 Hayek, M. N., Harwatt, H., Ripple, W. J., & Mueller, N. D. (2021). The carbon opportunity cost of  
731 animal-sourced food production on land. *Nature Sustainability*, *4*(1), 21–24.  
732 <https://doi.org/10.1038/s41893-020-00603-4>



- 733 Jiménez-Munoz, L., Torp Nielsen, M., Roman, L., & Corredig, M. (2023). Variation of in vitro  
734 digestibility of pea protein powder dispersions from commercially available sources. *Food*  
735 *Chemistry*, 401. <https://doi.org/10.1016/j.foodchem.2022.134178>
- 736 Johansson, M., Karkehabadi, S., Johansson, D. P., & Langton, M. (2023). Gelation behaviour and gel  
737 properties of the 7S and 11S globulin protein fractions from faba bean (*Vicia faba* var. *minor*) at  
738 different NaCl concentrations. *Food Hydrocolloids*, 142.  
739 <https://doi.org/10.1016/j.foodhyd.2023.108789>
- 740 Kamani, M. H., Liu, J., Fitzsimons, S. M., Fenelon, M. A., & Murphy, E. G. (2024). Determining the  
741 influence of fava bean pre-processing on extractability and functional quality of protein isolates.  
742 *Food Chemistry: X*, 21. <https://doi.org/10.1016/j.fochx.2024.101200>
- 743 Kaur, L., Mao, B., Beniwal, A. S., Abhilasha, Kaur, R., Chian, F. M., & Singh, J. (2022). Alternative  
744 proteins vs animal proteins: The influence of structure and processing on their gastro-small  
745 intestinal digestion. In *Trends in Food Science and Technology* (Vol. 122, pp. 275–286). Elsevier  
746 Ltd. <https://doi.org/10.1016/j.tifs.2022.02.021>
- 747 Kyriakopoulou, K., Dekkers, B., & van der Goot, A. J. (2019). Plant-Based Meat Analogues. In  
748 *Sustainable Meat Production and Processing* (pp. 103–126). Elsevier.  
749 <https://doi.org/10.1016/B978-0-12-814874-7.00006-7>
- 750 Lescinsky, H., Afshin, A., Ashbaugh, C., Bisignano, C., Brauer, M., Ferrara, G., Hay, S. I., He, J., Iannucci,  
751 V., Marczak, L. B., McLaughlin, S. A., Mullany, E. C., Parent, M. C., Serfes, A. L., Sorensen, R. J. D.,  
752 Aravkin, A. Y., Zheng, P., & Murray, C. J. L. (2022). Health effects associated with consumption of  
753 unprocessed red meat: a Burden of Proof study. *Nature Medicine*, 28(10), 2075–2082.  
754 <https://doi.org/10.1038/s41591-022-01968-z>
- 755 Liang, Y., Wong, S. S., Pham, S. Q., & Tan, J. J. (2016). Effects of globular protein type and  
756 concentration on the physical properties and flow behaviors of oil-in-water emulsions stabilized  
757 by micellar casein-globular protein mixtures. *Food Hydrocolloids*, 54, 89–98.  
758 <https://doi.org/10.1016/j.foodhyd.2015.09.024>
- 759 Lyu, Z., Sala, G., & Scholten, E. (2022). Water distribution in maize starch-pea protein gels as  
760 determined by a novel confocal laser scanning microscopy image analysis method and its effect  
761 on structural and mechanical properties of composite gels. *Food Hydrocolloids*, 133.  
762 <https://doi.org/10.1016/j.foodhyd.2022.107942>
- 763 Ma, K. K., Greis, M., Lu, J., Nolden, A. A., McClements, D. J., & Kinchla, A. J. (2022a). Functional  
764 Performance of Plant Proteins. In *Foods* (Vol. 11, Issue 4). MDPI.  
765 <https://doi.org/10.3390/foods11040594>
- 766 Ma, K. K., Greis, M., Lu, J., Nolden, A. A., McClements, D. J., & Kinchla, A. J. (2022b). Functional  
767 Performance of Plant Proteins. In *Foods* (Vol. 11, Issue 4). MDPI.  
768 <https://doi.org/10.3390/foods11040594>
- 769 Ma, K. K., Grossmann, L., Nolden, A. A., McClements, D. J., & Kinchla, A. J. (2022). Functional and  
770 physical properties of commercial pulse proteins compared to soy derived protein. *Future*  
771 *Foods*, 6. <https://doi.org/10.1016/j.fufo.2022.100155>
- 772 Magrini, M. B., Anton, M., Chardigny, J. M., Duc, G., Duru, M., Jeuffroy, M. H., Meynard, J. M., Micard,  
773 V., & Walrand, S. (2018). Pulses for Sustainability: Breaking Agriculture and Food Sectors Out of  
774 Lock-In. *Frontiers in Sustainable Food Systems*, 2. <https://doi.org/10.3389/fsufs.2018.00064>

- 775 Mazumder, M. A. R., Panpipat, W., Chaijan, M., Shetty, K., & Rawdkuen, S. (2023). Role of plant  
776 protein on the quality and structure of meat analogs: A new perspective for vegetarian foods. In  
777 *Future Foods* (Vol. 8). Elsevier B.V. <https://doi.org/10.1016/j.fufo.2023.100280>
- 778 McClements, D. J. (2023). Modeling the rheological properties of plant-based foods: Soft matter  
779 physics principles. *Sustainable Food Proteins*, 1(3), 101–132. <https://doi.org/10.1002/sfp2.1015>
- 780 McClements, D. J., & Grossmann, L. (2021). The science of plant-based foods: Constructing next-  
781 generation meat, fish, milk, and egg analogs. In *Comprehensive Reviews in Food Science and*  
782 *Food Safety* (Vol. 20, Issue 4, pp. 4049–4100). Blackwell Publishing Inc.  
783 <https://doi.org/10.1111/1541-4337.12771>
- 784 McClements, D. J., Newman, E., & McClements, I. F. (2019). Plant-based Milks: A Review of the  
785 Science Underpinning Their Design, Fabrication, and Performance. In *Comprehensive Reviews in*  
786 *Food Science and Food Safety* (Vol. 18, Issue 6, pp. 2047–2067). Blackwell Publishing Inc.  
787 <https://doi.org/10.1111/1541-4337.12505>
- 788 Michel, F., Hartmann, C., & Siegrist, M. (2021). Consumers' associations, perceptions and acceptance  
789 of meat and plant-based meat alternatives. *Food Quality and Preference*, 87.  
790 <https://doi.org/10.1016/j.foodqual.2020.104063>
- 791 Nagy, R., Máthé, E., Csapó, J., & Sipos, P. (2021). Modifying effects of physical processes on starch  
792 and dietary fiber content of foodstuffs. In *Processes* (Vol. 9, Issue 1, pp. 1–16). MDPI AG.  
793 <https://doi.org/10.3390/pr9010017>
- 794 Nicolai, T., & Chassenieux, C. (2019). Heat-induced gelation of plant globulins. In *Current Opinion in*  
795 *Food Science* (Vol. 27, pp. 18–22). Elsevier Ltd. <https://doi.org/10.1016/j.cofs.2019.04.005>
- 796 Okeudo-Cogan, M. C., Murray, B. S., Ettelaie, R., Connell, S. D., Radford, S. J., Micklethwaite, S., &  
797 Sarkar, A. (2023). Understanding the microstructure of a functional meat analogue:  
798 Demystifying interactions between fungal hyphae and egg white protein. *Food Hydrocolloids*,  
799 140. <https://doi.org/10.1016/j.foodhyd.2023.108606>
- 800 Osen, R., Toelstede, S., Wild, F., Eisner, P., & Schweiggert-Weisz, U. (2014). High moisture extrusion  
801 cooking of pea protein isolates: Raw material characteristics, extruder responses, and texture  
802 properties. *Journal of Food Engineering*, 127, 67–74.  
803 <https://doi.org/10.1016/j.jfoodeng.2013.11.023>
- 804 Paximada, P., Howarth, M., & Dubey, B. N. (2021). Double emulsions fortified with plant and milk  
805 proteins as fat replacers in cheese. *Journal of Food Engineering*, 288.  
806 <https://doi.org/10.1016/j.jfoodeng.2020.110229>
- 807 Ren, W., Xia, W., Gunes, D. Z., & Ahrné, L. (2024). Heat-induced gels from pea protein soluble  
808 colloidal aggregates: Effect of calcium addition or pH adjustment on gelation behavior and  
809 rheological properties. *Food Hydrocolloids*, 147.  
810 <https://doi.org/10.1016/j.foodhyd.2023.109417>
- 811 Schlangen, M., Taghian Dinani, S., Schutyser, M. A. I., & van der Goot, A. J. (2022a). Dry fractionation  
812 to produce functional fractions from mung bean, yellow pea and cowpea flour. *Innovative Food*  
813 *Science and Emerging Technologies*, 78. <https://doi.org/10.1016/j.ifset.2022.103018>

- 814 Schlangen, M., Taghian Dinani, S., Schutyser, M. A. I., & van der Goot, A. J. (2022b). Dry fractionation  
815 to produce functional fractions from mung bean, yellow pea and cowpea flour. *Innovative Food*  
816 *Science and Emerging Technologies*, 78. <https://doi.org/10.1016/j.ifset.2022.103018>
- 817 Schmid, E. M., Farahnaky, A., Adhikari, B., Savadkoobi, S., & Torley, P. J. (2024). Investigation into the  
818 physiochemical properties of soy protein isolate and concentrate powders from different  
819 manufacturers. *International Journal of Food Science and Technology*, 59(3), 1679–1693.  
820 <https://doi.org/10.1111/ijfs.16923>
- 821 Shrestha, S., Hag, L. van 't, Haritos, V., & Dhital, S. (2023). Rheological and textural properties of heat-  
822 induced gels from pulse protein isolates: Lentil, mungbean and yellow pea. *Food Hydrocolloids*,  
823 143. <https://doi.org/10.1016/j.foodhyd.2023.108904>
- 824 Sim, S. Y. J., Sriv, A., Chiang, J. H., & Henry, C. J. (2021). Plant proteins for future foods: A roadmap. In  
825 *Foods* (Vol. 10, Issue 8). MDPI AG. <https://doi.org/10.3390/foods10081967>
- 826 Snel, S. J. E., Bellwald, Y., van der Goot, A. J., & Beyrer, M. (2022). Novel rotating die coupled to a  
827 twin-screw extruder as a new route to produce meat analogues with soy, pea and gluten.  
828 *Innovative Food Science and Emerging Technologies*, 81.  
829 <https://doi.org/10.1016/j.ifset.2022.103152>
- 830 Stevenson, P. (2023). Links between industrial livestock production, disease including zoonoses and  
831 antimicrobial resistance. *Animal Research and One Health*, 1(1), 137–144.  
832 <https://doi.org/10.1002/aro2.19>
- 833 Sun, X. D., & Arntfield, S. D. (2012). Molecular forces involved in heat-induced pea protein gelation:  
834 Effects of various reagents on the rheological properties of salt-extracted pea protein gels. *Food*  
835 *Hydrocolloids*, 28(2), 325–332. <https://doi.org/10.1016/j.foodhyd.2011.12.014>
- 836 Tanger, C., Andlinger, D. J., Brümmer-Rolf, A., Engel, J., & Kulozik, U. (2021). Quantification of protein-  
837 protein interactions in highly denatured whey and potato protein gels. *MethodsX*, 8.  
838 <https://doi.org/10.1016/j.mex.2021.101243>
- 839 Tiernan, H., Byrne, B., & Kazarian, S. G. (2020). ATR-FTIR spectroscopy and spectroscopic imaging for  
840 the analysis of biopharmaceuticals. In *Spectrochimica Acta - Part A: Molecular and Biomolecular*  
841 *Spectroscopy* (Vol. 241). Elsevier B.V. <https://doi.org/10.1016/j.saa.2020.118636>
- 842 van der Sman, R. G. M., & van der Goot, A. J. (2023). Hypotheses concerning structuring of extruded  
843 meat analogs. In *Current Research in Food Science* (Vol. 6). Elsevier B.V.  
844 <https://doi.org/10.1016/j.crfs.2023.100510>
- 845 Weathers, S. T., Caviola, L., Scherer, L., Pfister, S., Fischer, B., Bump, J. B., & Jaacks, L. M. (2020).  
846 Quantifying the Valuation of Animal Welfare Among Americans. *Journal of Agricultural and*  
847 *Environmental Ethics*, 33(2), 261–282. <https://doi.org/10.1007/s10806-020-09824-1>
- 848 Wittek, P., Zeiler, N., Karbstein, H. P., & Emin, M. A. (2020). Analysis of the complex rheological  
849 properties of highly concentrated proteins with a closed cavity rheometer. *Applied Rheology*,  
850 30(1), 64–76. <https://doi.org/10.1515/arh-2020-0107>
- 851 Xia, W., Siu, W. K., & Sagis, L. M. C. (2021). Linear and non-linear rheology of heat-set soy protein  
852 gels: Effects of selective proteolysis of  $\beta$ -conglycinin and glycinin. *Food Hydrocolloids*, 120.  
853 <https://doi.org/10.1016/j.foodhyd.2021.106962>

- 854 Xia, W., Zhu, L., Delahaije, R. J. B. M., Cheng, Z., Zhou, X., & Sagis, L. M. C. (2022). Acid-induced gels  
855 from soy and whey protein thermally-induced mixed aggregates: Rheology and microstructure.  
856 *Food Hydrocolloids*, 125. <https://doi.org/10.1016/j.foodhyd.2021.107376>
- 857 Yang, J., Lorenzetti, R. L., Bing, D., Zhang, S., Lu, J., & Chen, L. (2023). Composition, functionalities,  
858 and digestibility of proteins from high protein and normal pea ( *Pisum sativum* ) genotypes .  
859 *Sustainable Food Proteins*, 1(1), 4–15. <https://doi.org/10.1002/sfp2.1005>
- 860 Zhao, J., Cui, J. K., Chen, R. X., Tang, Z. Z., Tan, Z. L., Jiang, L. Y., & Liu, F. (2021). Real-time in-situ  
861 quantification of protein secondary structures in aqueous solution based on ATR-FTIR  
862 subtraction spectrum. *Biochemical Engineering Journal*, 176.  
863 <https://doi.org/10.1016/j.bej.2021.108225>
- 864
- 865

## **Gelation and Rheological Properties of Ultrasound-Extracted Faba Bean Protein: A Comparative Study with Commercial Plant Proteins**

**Abraham Badjona<sup>1</sup>, Beatrice Cheronob<sup>1</sup> Robert Bradshaw<sup>2</sup>, Bipro Dubey<sup>1,3\*</sup>**

<sup>1</sup>National Centre of Excellence for Food Engineering, Sheffield Hallam University, Sheffield, S1 1WB, [a.badjona@shu.ac.uk](mailto:a.badjona@shu.ac.uk) (A.B), [beatricecheronob@gmail.com](mailto:beatricecheronob@gmail.com), [b.dubey@shu.ac.uk](mailto:b.dubey@shu.ac.uk) (B.D)

<sup>2</sup>Bimolecular Research Centre, Sheffield Hallam University, Sheffield, S1 1WB, UK; [r.bradshaw@shu.ac.uk](mailto:r.bradshaw@shu.ac.uk) (R.B)

<sup>3</sup>School of Engineering and Built Environment, College of Business, Technology and Engineering, Sheffield Hallam University, Sheffield, S1 1WB, UK.

\*Correspondence: [b.dubey@shu.ac.uk](mailto:b.dubey@shu.ac.uk) (B.D)

### Highlights

- Ultrasound extracted faba bean protein (US-FBP) was assessed and compared to commercial plant proteins (Soy and Pea).
- US-FBP and commercial plant proteins viscosity showed different shear thinning behavior and fitted with power law model.
- In situ gelation showed major differences in gel formation mechanism
- The gel strength, water holding capacity profile and viscoelastic properties of US-FBP were different from commercial proteins.
- Major structural differences were observed between lab extracted proteins and commercial proteins.

**Declaration of interests**

The authors declare that they have no known competing financial interests or personal relationships that could have appeared to influence the work reported in this paper.

The author is an Editorial Board Member/Editor-in-Chief/Associate Editor/Guest Editor for *[Journal name]* and was not involved in the editorial review or the decision to publish this article.

The authors declare the following financial interests/personal relationships which may be considered as potential competing interests:

Journal Pre-proof